Astrid Ayala, Szabolcs Blazsek and Alvaro Escribano*

Anticipating extreme losses using score-driven shape filters

https://doi.org/10.1515/snde-2021-0102
Received November 24, 2021; accepted August 21, 2022; published online October 10, 2022

Abstract: We suggest a new value-at-risk (VaR) framework using EGARCH (exponential generalized autoregressive conditional heteroskedasticity) models with score-driven expected return, scale, and shape filters. We use the EGB2 (exponential generalized beta of the second kind), NIG (normal-inverse Gaussian), and Skew-Gen-*t* (skewed generalized-*t*) distributions, for which the score-driven shape parameters drive the skewness, tail shape, and peakedness of the distribution. We use daily data on the Standard & Poor's 500 (S&P 500) index for the period of February 1990 to October 2021. For all distributions, likelihood-ratio (LR) tests indicate that several EGARCH models with dynamic shape are superior to the EGARCH models with constant shape. We compare the realized volatility with the conditional volatility estimates, and we find two Skew-Gen-*t* specifications with dynamic shape, which are superior to the Skew-Gen-*t* specification with constant shape. The shape parameter dynamics are associated with important events that affected the stock market in the United States (US). VaR backtesting is performed for the dot.com boom (January 1997 to October 2020), the 2008 US Financial Crisis (October 2007 to March 2009), and the coronavirus disease (COVID-19) pandemic (January 2020 to October 2021). We show that the use of the dynamic shape parameters improves the VaR measurements.

Keywords: dynamic conditional score (DCS); generalized autoregressive score (GAS); score-driven shape parameters; value-at-risk (VaR); VaR backtesting.

JEL Classification: C22; C52; C58.

1 Introduction

When conditional probability distributions that include scale and shape parameters are estimated for financial returns, then all those parameters influence volatility. A leading example of the use of those distributions for volatility modeling is the Student's *t*-distribution (Bollerslev 1987), in which the degrees of freedom parameter influences the tail shape of the distribution. The scale parameters are dynamic in all classical volatility models (e.g. Engle 1982; Bollerslev 1986, 1987; Nelson 1991; Harvey, Ruiz, and Shephard 1994), but the shape parameters are constant (or not used) in most of those models. The dynamic modeling of the shape parameters is practically relevant, because the tail shape of the conditional probability distribution varies over time, and the dynamic models of tail shape may anticipate extreme losses on portfolios, or they may improve the pricing of financial derivatives.

Studies in the body of literature on the tail shape dynamics of financial returns use several econometric methods and statistical tests. An important paper is the work of Hansen (1994), in which the Skew-Gen-*t*

***Corresponding author: Alvaro Escribano**, Department of Economics, Universidad Carlos III de Madrid, Getafe, 28903, Spain, E-mail: alvaroe@eco.uc3m.es
Astrid Ayala and Szabolcs Blazsek, School of Business, Universidad Francisco Marroquín, Ciudad de Guatemala, 01010, Guatemala

(skewed generalized-*t*) distribution with dynamic degrees of freedom and skewness parameters is used, and which we extend in the present paper. Dynamic shape parameters are also considered in the work of Quintos, Fan, and Phillips (2001), which suggests tests of tail shape constancy that are later applied in the work of Galbraith and Zernov (2004). Similarly, the work of Bollerslev and Todorov (2011) focuses on the tail-behavior of the probability distribution by suggesting a nonparametric method for estimating the jump tails of Itô semimartingale processes. Those works focus on the tail-behavior and the statistical tests allow an unknown breakpoint. A contribution of our work, with respect to the statistical method of Quintos, Fan, and Phillips (2001), Galbraith and Zernov (2004), and Bollerslev and Todorov (2011), is that in the present work the whole probability distribution is modeled (and not just of the tail). Using panel data models, Kelly and Jiang (2014) identify a common variation in the tail shape of United States (US) stock returns. Those authors note that dynamic tail risk estimates are infeasible in a univariate time series model due to the infrequent nature of outliers. For this reason, they use a panel estimation approach that captures common variation in the tail risks of individual firms. In the present paper, we suggest a feasible univariate time series model which provides dynamic tail risk estimates by using information on the whole probability distribution. In addition, options data for the estimation of dynamic tail shape are used in several works in the body of literature (e.g. Bakshi, Kapadia, and Madan 2003; Bollerslev, Tauchen, and Zhou 2009; Backus, Chernov, and Martin 2011; Bollerslev and Todorov 2014; Bollerslev, Todorov, and Xu 2015). Nevertheless, options data may not be available for the all financial assets for which tail shape dynamics are estimated. The econometric method of the present paper directly uses the time series financial asset returns for the estimation of tail shape dynamics.

As aforementioned, we extend the work of Hansen (1994), by suggesting score-driven dynamics for the location, scale, and shape for the Skew-Gen-*t* distribution. Score-driven time series models are introduced in the works of Creal, Koopman, and Lucas (2008, 2011, 2013), Harvey and Chakravarty (2008), and Harvey (2013). All score-driven filters are observation-driven models (Cox 1981), which are updated by using the partial derivatives of the log conditional density of the dependent variable with respect to dynamic parameters (Harvey 2013). The updating terms are named score functions. In the work of Blasques, Koopman, and Lucas (2015), it is shown for univariate score-driven filters, such as Beta-*t*-EGARCH, that a score-driven update of a time series model, asymptotically and in expectation at the true values of the parameters, reduces the Kullback–Leibler distance at every step. The authors show that only score-driven updates have this property. The work of Blasques, Lucas, and van Vlodrop (2020) presents simulation-based results, which also support the use of the score-driven models for finite samples.

In this paper, news on asset value updates volatility not only through scale but also shape, because the conditional volatility filters of this paper depend on dynamic scale and dynamic shape parameters. We extend the model of Blazsek and Monteros (2017), which to the best of our knowledge is the first paper in the literature with score-driven shape parameters, in which the use of the Beta-*t*-EGARCH (exponential autoregressive generalized conditional heteroskedasticity) model (Harvey and Chakravarty 2008) with a score-driven degrees of freedom parameter is suggested. We also refer to a previous version of the present paper, Ayala, Blazsek, and Escribano (2019), in which the idea of the extension of the model of Blazsek and Monteros (2017) and some preliminary results are presented.

The issue of modelling the shape parameter is also addressed in other recent papers in the literature on score-driven models. The works of Massacci (2017) and Schwaab, Zhang, and Lucas (2020) use an extreme value theory approach to model the tail of the conditional distribution of financial returns. In the work of Schwaab, Zhang, and Lucas (2020), tail shape dynamics are modeled by using a two-step estimation procedure for the generalized Pareto distribution with score-driven shape parameters. In the present paper, the score-driven tail shape, skewness, and peakedness of financial returns are estimated in one step. The major contribution of the present work, with respect to the papers of Massacci (2017) and Schwaab, Zhang, and Lucas (2020), is that we model the shape parameter of the whole distribution (and not just of the tail). Due to this point, our paper can be seen as an extension of the work of Hansen (1994), and also an improvement of the econometric methods of Massacci (2017) and Schwaab, Zhang, and Lucas (2020), providing an elegant representation of tail shape dynamics for financial returns.

We use the EGB2 (exponential generalized beta of the second kind) (Caivano and Harvey 2014), NIG (normal-inverse Gaussian) (Barndorff-Nielsen and Halgreen 1977), and Skew-Gen-*t* (McDonald and Michelfelder 2017) distributions with dynamic location, scale, and shape parameters. Thus, we extend the works on score-driven EGARCH models with constant shape parameters from the literature (e.g. Harvey 2013; Caivano and Harvey 2014; Harvey and Sucarrat 2014; Harvey and Lange 2017). We present technical details of the score-driven EGARCH with dynamic shape parameters models for all probability distributions, and we also present the score functions which update the score-driven filters in closed form. The score-driven models are estimated by using the maximum likelihood (ML) method, and we present the stochastic properties of the score functions. For each score-driven specification, the correct specification of the probability distributions of financial returns is tested up to the fourth conditional moment, by using the martingale difference sequence (MDS) test of Escanciano and Lobato (2009). The consistency of the ML estimator of the score-driven shape filters is also studied, by performing Monte Carlo (MC) simulation experiments for known data generating processes.

For control data, daily log-return time series observations are used from the Standard & Poor's 500 (S&P 500) index for the period of February 14, 1990 to October 21, 2021. The application of the S&P 500 data is relevant, for example, for investors of (i) well-diversified US equity portfolios, (ii) S&P 500 futures and options contracts, and (iii) exchange traded funds (ETFs) related to the S&P 500 index. The full sample period includes data for three periods with high stock market volatility and extreme observations: (i) dot.com boom (January 2, 1997 to October 9, 2002), (ii) 2008 US Financial Crisis (October 1, 2007 to March 31, 2009), and (iii) part of the coronavirus disease (COVID-19) pandemic (January 9, 2020 until the end of the sample period, i.e. October 21, 2021).

An advantage of the use of the EGB2, NIG, and Skew-Gen-*t* probability distributions is their flexibility, by which they can capture asymmetric features of the probability distribution of returns, and they can also set heavy tails for the distribution to capture possible extreme observations. Motivated by the literature, we estimate all EGARCH models with score-driven expected return and score-driven volatility with leverage effects (Harvey 2013). Moreover, with respect to the shape parameters of the distributions, we estimate all possible combinations of time-invariant and dynamic (i.e. score-driven) shape parameters, to find the correct specification of the shape parameters for each distribution.

The statistical performances of alternative score-driven models are compared by using likelihood-ratio (LR) tests, which indicate that several specifications with score-driven shape are superior to the score-driven models with constant shape. The LR tests are performed for the periods of February 14, 1990 to October 21, 2021 and January 3, 2000 to October 21, 2021. The use of the chi-squared distribution-based LR test is valid for the score-driven models of this paper, because the score-driven models with constant shape are special cases of the score-driven models with dynamic shape.

The volatility estimates for the score-driven models are compared with the 5 min realized volatility, where the use of the latter as a proxy of true volatility is motivated by the works of Liu, Patton, and Sheppard (2015) and Harvey and Lange (2018). With respect to realized volatility, we also refer to the seminal works of Andersen and Bollerslev (1998) and Hansen and Lunde (2006). We use the squared error (SE) and absolute error (AE) loss functions, to compare the realized volatility with the estimated volatility for each model. Realized volatility data are for the period of January 3, 2000 to October 21, 2021, for which realized volatility of the S&P 500 is available. Based on the loss functions, a robust in-sample volatility forecasting accuracy comparison test indicates the superiority of two dynamic shape specifications for the Skew-Gen-*t* distribution.

VaR forecasting performances of the score-driven Skew-Gen-*t* with constant and dynamic shape specifications are compared. For the score-driven EGARCH model with dynamic shape all shape parameters are score-driven. VaR forecasting is performed for the periods of the dot.com boom, 2008 US Financial Crisis, and COVID-19 pandemic, by using 99% confidence level and 1 day time horizon MC-VaR estimates. For VaR backtesting, we use the Kupiec test (Kupiec 1995), the Christoffersen test (Christoffersen 1998), and the framework of the Basel Committee (1996), which indicate that the VaR measurement performance of the Skew-Gen-*t* with dynamic shape specification is superior to that of the score-driven Skew-Gen-*t* with constant shape specification for all backtesting periods.

The in-sample statistical performance results, the in-sample volatility forecasting performance results, and the out-of-sample VaR backtesting results suggest that the score-driven EGARCH with dynamic shape parameters is superior to the score-driven EGARCH with constant shape parameters. This may motivate the practical application of the extended score-driven shape specifications for the anticipation of extreme losses in the US stock market. The remainder of this paper is organized as follows: Section 2 presents the econometric tool of the new method. Section 3 describes the control data. Section 4 presents the method implementation and results. Section 5 concludes.

2 Econometric tool of the new method

2.1 Econometric models with score-driven shape parameter filters

The score-driven models of the daily log-return of the S&P 500 index y_t are formulated as:

$$y_t = \mu_t + \upsilon_t = \mu_t + \exp(\lambda_t)\epsilon_t \tag{1}$$

where μ_t and $\exp(\lambda_t)$ are the location and scale parameters, respectively. The error term ϵ_t is specified according to the following conditional distributions: (i) $\epsilon_t|\mathcal{F}_{t-1} \sim \text{EGB2}[0, 1, \exp(\xi_t), \exp(\zeta_t)]$. If $\xi_t = \zeta_t$ then the probability distribution is symmetric, if $\xi_t > \zeta_t$ then the probability distribution is skewed to the right, and if $\xi_t < \zeta_t$ then the probability distribution is skewed to the left. Different values of ξ_t and ζ_t may imply tail-thickness on the left or right side of the probability distribution. For this conditional distribution all moments are finite, and the log of the conditional density of y_t is:

$$\begin{aligned} \ln\ f(y_t|\mathcal{F}_{t-1};\Theta) = {} & \exp(\xi_t)\epsilon_t - \lambda_t - \ln\Gamma[\exp(\xi_t)] - \ln\Gamma[\exp(\zeta_t)] \\ & + \ln\Gamma[\exp(\xi_t) + \exp(\zeta_t)] - [\exp(\xi_t) + \exp(\zeta_t)]\ln[1 + \exp(\epsilon_t)] \end{aligned} \tag{2}$$

where $\Gamma(x)$ is the gamma function. (ii) $\epsilon_t|\mathcal{F}_{t-1} \sim \text{NIG}[0, 1, \exp(\nu_t), \exp(\nu_t)\tanh(\eta_t)]$, where $\tanh(x)$ is the hyperbolic tangent function, and the absolute value of parameter $\exp(\nu_t)\tanh(\eta_t)$ is less than parameter $\exp(\nu_t)$, as required for NIG. For this error term ν_t controls for tail-thickness. Moreover, if $\eta_t = 0$ then the probability distribution is symmetric, if $\eta_t > 0$ then the probability distribution is skewed to the right, and if $\eta_t < 0$ then the probability distribution is skewed to the left. For this conditional distribution all moments are finite, and the log of the conditional density of y_t is:

$$\begin{aligned} \ln\ f(y_t|\mathcal{F}_{t-1};\Theta) = {} & \nu_t - \lambda_t - \ln(\pi) + \exp(\nu_t)\left[1 - \tanh^2(\eta_t)\right]^{1/2} \\ & + \exp(\nu_t)\tanh(\eta_t)\epsilon_t + \ln K^{(1)}\left[\exp(\nu_t)\sqrt{1+\epsilon_t^2}\right] - \frac{1}{2}\ln\left(1+\epsilon_t^2\right) \end{aligned} \tag{3}$$

where $K^{(1)}(x)$ is the modified Bessel function of the second kind of order 1. (iii) The third probability distribution is $\epsilon_t|\mathcal{F}_{t-1} \sim \text{Skew}-\text{Gen}-t[0, 1, \tanh(\tau_t), \exp(\nu_t) + 4, \exp(\eta_t)]$, where the degrees of freedom parameter, $\exp(\nu_t) + 4$, is higher than four. For this error term, ν_t controls for tail-thickness and η_t controls for the peakedness of the center of the probability distribution. Moreover, if $\tau_t = 0$ then the probability distribution is symmetric, if $\tau_t > 0$ then the probability distribution is skewed to the right, and if $\tau_t < 0$ then the probability distribution is skewed to the left. For this conditional distribution the fourth moment is finite, and the log of the conditional density of y_t is:

$$\ln f(y_t|\mathcal{F}_{t-1};\Theta) = \eta_t - \lambda_t - \ln(2) - \frac{\ln[\exp(\nu_t)+4]}{\exp(\eta_t)} - \ln\Gamma\left[\frac{\exp(\nu_t)+4}{\exp(\eta_t)}\right] - \ln\Gamma[\exp(-\eta_t)] + \ln\Gamma\left[\frac{\exp(\nu_t)+5}{\exp(\eta_t)}\right] - \frac{\exp(\nu_t)+5}{\exp(\eta_t)}\ln\left\{1+\frac{|\epsilon_t|^{\exp(\eta_t)}}{[1+\tanh(\tau_t)\,\mathrm{sgn}(\epsilon_t)]^{\exp(\eta_t)}\times[\exp(\nu_t)+4]}\right\} \tag{4}$$

where sgn(x) is the signum function. The density functions for the EGB2, NIG, and Skew-Gen-t distributions with alternative shape parameters are presented in Figure 1. Further technical details for each distribution are presented in Appendix A.

For the shape parameters, we use the general notation $\rho_{k,t}$ for $k = 1, \ldots, K$, for each distribution. For example, EGB2 $[0, 1, \exp(\xi_t), \exp(\zeta_t)]$ = EGB2 $[0, 1, \exp(\rho_{1,t}), \exp(\rho_{2,t})]$, where $K = 2$ is the number of shape parameters. In the specifications of the conditional distributions of ϵ_t, we use $\mathcal{F}_{t-1} = [\mu_1, \lambda_1, (\rho_{1,1}, \ldots, \rho_{K,1}), (y_1, \ldots, y_{t-1})]$, i.e. we condition on the initial values of all filters.

In the following, the score-driven filters for μ_t, λ_t, and $\rho_{k,t}$ are presented. First, μ_t is specified as:

$$\mu_t = c + \phi\mu_{t-1} + \theta u_{\mu,t-1} \tag{5}$$

where $|\phi| < 1$ and $u_{\mu,t}$ is the scaled score function of the log-likelihood (LL) with respect to μ_t (Appendix A and Section 2.4). The score-driven filter for μ_t is named the first-order quasi-autoregressive QAR (1) model (Harvey 2013). Second, λ_t is specified as:

$$\lambda_t = \omega + \beta\lambda_{t-1} + \alpha u_{\lambda,t-1} + \alpha^* \,\mathrm{sgn}(-\epsilon_{t-1})(u_{\lambda,t-1}+1) \tag{6}$$

where $|\beta| < 1$, $u_{\lambda,t}$ is the score function of the LL with respect to λ_t (Appendix A and Section 2.4). This specification measures leverage effects (Black 1976), by using parameter α^* in the score-driven EGARCH model

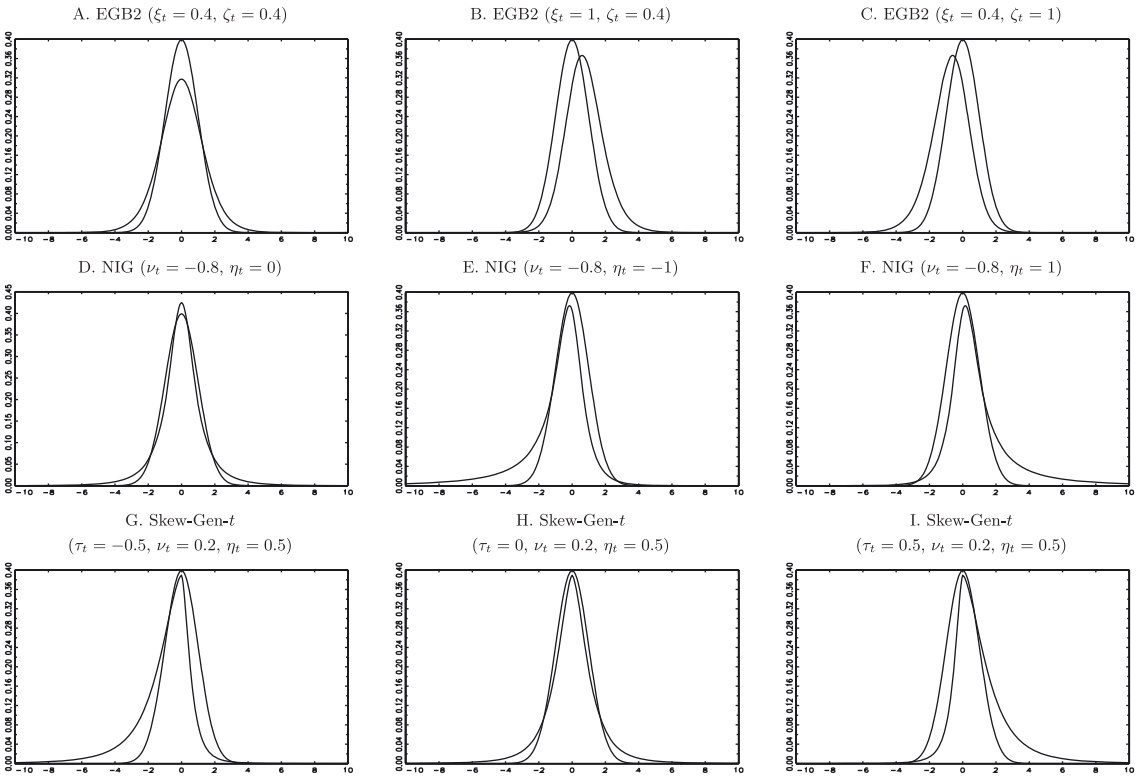

Figure 1: Density functions for the EGB2, NIG, Skew-Gen-t (thick lines), and standard normal (thin lines) distributions.

(Harvey 2013). The score-driven EGARCH models with constant shape parameters that use EGB2, NIG, and Skew-Gen-t distributions are named EGB2-EGARCH (Caivano and Harvey 2014), NIG-EGARCH (Blazsek, Ho, and Liu 2018), and Beta-Skew-Gen-t-EGARCH (Harvey and Lange 2017), respectively. Third, $\rho_{k,t}$ is specified as:

$$\rho_{k,t} = \delta_k + \gamma_k \rho_{k,t-1} + \kappa_k u_{\rho,k,t-1} \tag{7}$$

where $|\gamma_k| < 1$, and $u_{\rho,k,t}$ is the score function of the LL with respect to $\rho_{k,t}$ (Appendix A and Section 2.4). For each distribution the constant shape parameter model, i.e. $\rho_{k,t} = \delta_k$, is used as the benchmark, which we name the econometric tool of the existing method. Lags of exogenous explanatory variables may also be included in Eqs. (5)–(7), to extend the models of this paper.

Different ways of initialization are considered for the filters. For the results reported in the present paper, μ_t is initialized by using pre-sample data, λ_t by using parameter λ_0, and $\rho_{k,t}$ by using its unconditional mean $\delta_k/(1-\gamma_k)$. Nevertheless, the results of this paper are robust to other ways of initialization. For example, the results for the case where parameters μ_0 and $\rho_{k,0}$ were used in this study for the initialization of μ_t and $\rho_{k,t}$ are similar to the results reported in this paper.

Finally, we refer to the following two model specifications, which we studied as alternatives to the specifications of this section. First, we studied two-component λ_t filters, motivated by the work of Harvey and Lange (2018), in which two-component score-driven volatility models are suggested with time-invariant shape parameters. Second, we also studied multivariate filters involving the vector $(\mu_t, \lambda_t, \rho_{1,t}, \dots, \rho_{K,t})'$, motivated by the work of Blazsek, Escribano, and Licht (2022), in which multivariate score-driven filters are suggested for $(\mu_t, \lambda_t)'$ with time-invariant shape parameters. For both alternatives, we find that the ML estimates are not reliable due to numerical problems in the maximization of the LL function. Hence, the results for those alternatives are not reported.

2.2 ML estimator

All models of this paper are estimated by using the ML method:

$$\hat{\Theta} = \arg\max_{\Theta} \mathrm{LL}(y_1, \dots, y_T; \Theta) = \arg\max_{\Theta} \frac{1}{T} \sum_{t=1}^{T} \ln\, f(y_t|\mathcal{F}_{t-1}; \Theta) \tag{8}$$

where $\Theta = (\Theta_1, \dots, \Theta_S)'$ is the vector of time-invariant parameters, and $\ln\, f(y_t|\mathcal{F}_{t-1}; \Theta)$ for the EGB2, NIG, and Skew-Gen-t probability distributions is presented in Appendix A.

The $T \times S$ matrix of contributions to the gradient $G\,(y_1, \dots, y_T;\ \Theta)$ is defined by its elements:

$$G_{t,i}(\Theta) = -\frac{\partial\, \ln\, f(y_t|\mathcal{F}_{t-1}; \Theta)}{\partial \Theta_i} \tag{9}$$

for period $t = 1, \dots, T$, and parameter $i = 1, \dots, S$ (Wooldridge 1994). The tth row of $G\,(y_1, \dots, y_T;\ \Theta)$ is denoted by using $G_t(\Theta)$, which is the score vector for the tth observation. The asymptotic covariance matrix of $\hat{\Theta}$ is estimated by using the information matrix $\left\{(1/T)\sum_{t=1}^{T}\left[G_t(\hat{\Theta})' G_t(\hat{\Theta})\right]\right\}^{-1}$ (Blasques et al. 2022; Creal, Koopman, and Lucas 2013; Harvey 2013). We use the following maintained assumptions:

(S1) Asymptotically, $f(y_t|\mathcal{F}_{t-1}; \Theta_0) = p_0(y_t|\mathcal{F}_{t-1}; \Theta_0)$ for Θ_0 from the parameter set $\tilde{\Theta} \subset \mathbb{R}^S$, where p_0 is the true conditional density, and Θ_0 represents the true values of Θ.

(S2) Asymptotically, $f(y_t|\mathcal{F}_{t-1}; \Theta_0)$ is a dynamically complete density (Wooldridge 1994).

(S3) For all $\Theta \in \tilde{\Theta}$, $|\lambda_t| < \lambda_{\max} < \infty$, and $|\rho_{k,t}| < \rho_{k,max} < \infty$

for all t and k, where $\lambda_{\max} \in \mathbb{R}^+$ and $\rho_{k,\,\max} \in \mathbb{R}^+$ do not depend on ϵ_t for all t. (S1) assumes an asymptotically correct model specification, which is studied empirically by using the specification tests of Section 2.3. (S2) assumes that the dynamics of the dependent variable are asymptotically correctly formulated for each period. One of the consequences of (S2) is that, asymptotically, $G_t(\Theta_0)'$ is a MDS (Wooldridge 1994). (S3) assumes the uniform boundedness of the log-scale and all shape parameters, which implies finite moments for the score

functions. (S2) and (S3) have consequences on the properties of the score functions of dynamic parameters (Section 2.4).

2.3 Specification tests

We empirically study assumption (S1) for the first four conditional moments for each score-driven model. The first four conditional moments of ϵ_t for the EGB2, NIG, and Skew-Gen-t distributions are reported in Appendix A. We define the following auxiliary error term as:

$$\epsilon_t^* = \frac{\epsilon_t - E(\epsilon_t|\mathcal{F}_{t-1};\Theta)}{\mathrm{Var}^{1/2}(\epsilon_t|\mathcal{F}_{t-1};\Theta)} = \frac{\epsilon_t - E(\epsilon_t|\epsilon_1,\ldots,\epsilon_{t-1};\Theta)}{\mathrm{Var}^{1/2}(\epsilon_t|\epsilon_1,\ldots,\epsilon_{t-1};\Theta)} \tag{10}$$

This transformation reduces the importance of those outliers that appear within ϵ_t. The robustness of model specification tests is increased when residuals are standardized according to Eq. (10) (see Li 2004, Chapter 4). The model specification test of the present paper uses the following properties:

$$E\left(\epsilon_t^*|\mathcal{F}_{t-1};\Theta\right) = E\left(\epsilon_t^*|\epsilon_1^*,\ldots,\epsilon_{t-1}^*;\Theta\right) = 0 \tag{11}$$

$$E\left[\left(\epsilon_t^*\right)^2 - 1|\mathcal{F}_{t-1};\Theta\right] = E\left[\left(\epsilon_t^*\right)^2 - 1|\epsilon_1^*,\ldots,\epsilon_{t-1}^*;\Theta\right] = 0 \tag{12}$$

$$E\left[\left(\epsilon_t^*\right)^3 - \mathrm{Skew}(\epsilon_t|\mathcal{F}_{t-1})|\mathcal{F}_{t-1};\Theta\right] = E\left[\left(\epsilon_t^*\right)^3 - \mathrm{Skew}(\epsilon_t|\mathcal{F}_{t-1})|\epsilon_1^*,\ldots,\epsilon_{t-1}^*;\Theta\right] = 0 \tag{13}$$

$$E\left[\left(\epsilon_t^*\right)^4 - \mathrm{Kurt}(\epsilon_t|\mathcal{F}_{t-1})|\mathcal{F}_{t-1};\Theta\right] = E\left[\left(\epsilon_t^*\right)^4 - \mathrm{Kurt}(\epsilon_t|\mathcal{F}_{t-1})|\epsilon_1^*,\ldots,\epsilon_{t-1}^*;\Theta\right] = 0 \tag{14}$$

The random variables within the expectations of Eqs. (11)–(14) are MDSs, which is tested by using the MDS test of Escanciano and Lobato (2009) for all model specifications of our paper. The rejection of the MDS null hypothesis of the Escanciano–Lobato test for any of the conditional moments of Eqs. (11)–(14) is evidence against the correct model specification assumption (S1).

2.4 Score functions

We present the asymptotic properties of the score functions $u_{\mu,t}$, $u_{\lambda,t}$, and $u_{\rho,k,t}$ at $\Theta = \Theta_0$.

First, we prove that all score functions, asymptotically at the true values of parameters, are MDSs. Score function $u_{\mu,t}$, asymptotically at the true values of parameters, is a MDS due to the following arguments. Due to (S2), $G_t\,(\Theta_0)'$, asymptotically, is a MDS:

$$E_{t-1}\left[\frac{\partial\ \ln\ f(y_t|\mathcal{F}_{t-1},\Theta)}{\partial\Theta'}\right] = E_{t-1}\left[\frac{\partial\ \ln\ f(y_t|\mathcal{F}_{t-1},\Theta)}{\partial\mu_t}\right] \times \frac{\partial\mu_t}{\partial\Theta'} = 0 \tag{15}$$

where index $t-1$ indicates expectations that are conditional on $\mathcal{F}_{t-1}$. Since $\left(\partial\mu_t/\partial\Theta'\right) \neq 0$,

$$E_{t-1}\left[\frac{\partial\ \ln\ f(y_t|\mathcal{F}_{t-1},\Theta)}{\partial\mu_t}\right] = E_{t-1}\left(k_t \times u_{\mu,t}\right) = E_{t-1}(u_{\mu,t}) \times k_t = 0 \tag{16}$$

where k_t is defined in Appendix A for each distribution. Thus, $E_{t-1}\,(u_{\mu,t}) = 0$. Score function $u_{\lambda,t}$, asymptotically at the true values of parameters, is a MDS due to the following arguments. Due to (S2), asymptotically, $G_t\,(\Theta_0)'$ is a MDS:

$$E_{t-1}\left[\frac{\partial\ \ln\ f(y_t|\mathcal{F}_{t-1},\Theta)}{\partial\Theta'}\right] = E_{t-1}\left[\frac{\partial\ \ln\ f(y_t|\mathcal{F}_{t-1},\Theta)}{\partial\lambda_t}\right] \times \frac{\partial\lambda_t}{\partial\Theta'} = 0 \tag{17}$$

Since $\left(\partial\lambda_t/\partial\Theta'\right) \neq 0$,

$$E_{t-1}\left[\frac{\partial\ \ln\ f(y_t|\mathcal{F}_{t-1},\Theta)}{\partial\lambda_t}\right] = E_{t-1}(u_{\lambda,t}) = 0 \tag{18}$$

Score functions $u_{\rho,k,t}$ for $k = 1, \dots, K$, asymptotically at the true values of parameters, are MDSs because, due to (S2), $G_t\ (\Theta_0)'$, asymptotically, is a MDS:

$$E_{t-1}\left[\frac{\partial \ln f(y_t|\mathcal{F}_{t-1}, \Theta)}{\partial \Theta'}\right] = E_{t-1}\left[\frac{\partial \ln f(y_t|\mathcal{F}_{t-1}, \Theta)}{\partial \rho_{k,t}}\right] \times \frac{\partial \rho_{k,t}}{\partial \Theta'} = 0 \tag{19}$$

Since $\left(\partial \rho_{k,t}/\partial \Theta'\right) \neq 0$,

$$E_{t-1}\left[\frac{\partial \ln f(y_t|\mathcal{F}_{t-1}, \Theta)}{\partial \rho_{k,t}}\right] = E_{t-1}(u_{\rho,k,t}) = 0 \tag{20}$$

Hence, $E(u_{\mu,t}) = 0$, $E(u_{\lambda,t}) = 0$, and $E(u_{\rho,k,t}) = 0$, asymptotically at the true values of parameters, due to the law of iterated expectations.

Second, we prove the finiteness of the second moments and covariances of the score functions and their derivatives, which is needed for the finiteness of the elements of the information matrix. The following results are true for all $\Theta \in \tilde{\Theta}$.

The score-driven models are robust to extreme observations, because the score functions in those models reduce the effects of outliers on the location, scale, and shape filters. Hence, outliers appear within the error term ϵ_t rather than within the score functions that update the dynamic equations. By using the S&P 500 dataset, the outlier transformation of the score functions is presented in Figure 2, which shows that extreme observations are never accentuated by the location, scale, and shape score functions. According to the figure, the transformations of ϵ_t asymptotically go to zero, are linear, or are in accordance with a slowly increasing function (e.g. the natural logarithm function $\ln(x)$).

In Appendix B, the derivatives of $u_{\mu,t}$, $u_{\lambda,t}$, and $u_{\rho,k,t}$ for $k = 1, \dots, K$, with respect to μ_t, λ_t, and $\rho_{k,t}$ for $k = 1, \dots, K$ are presented. Figures B1–B3 indicate that the derivatives of each score-function go to zero, are linear, or are slowly increasing functions as $|\epsilon_t| \to \infty$. In the illustrations of the score functions and their derivatives, the unconditional mean estimates of the score-driven variables are used, but the same functional forms of the score functions and their derivatives hold if the score-driven variables are replaced by their finite boundaries in accordance with (S3).

The score functions and their derivatives are nonlinear transformations of ϵ_t, for which the highest rate of increase is a linear increase, as $|\epsilon_t| \to \infty$ (Figures 2 and B1–B3).

This implies that, for the second moments and covariances of the score functions and their derivatives, the highest rate of increase of the squared score function or its derivative is a quadratic increase, as $|\epsilon_t| \to \infty$. For EGB2 and NIG all moments of ϵ_t are finite, and for Skew-Gen-t we assume that the fourth moment is finite. Hence, there exist positive numbers a and b that define the intervals $(-\infty, -a]$ and $[b, \infty)$, respectively, for which the integrands of the fourth moment of ϵ_t bound the integrands of the second moments and covariances of all score functions and their derivatives. This implies that the variances and the covariances of all score functions and their second moments are finite for all score-driven models of this paper.

Third, scaled score function, asymptotically at the true values of parameters, $u_{\mu,t}$ is white noise, because $u_{\mu,t}$, asymptotically, is a MDS and $\text{Var}(u_{\mu,t}) < \infty$. Score function $u_{\lambda,t}$, asymptotically at the true values of parameters, is white noise, because $u_{\lambda,t}$, asymptotically, is a MDS and $\text{Var}(u_{\lambda,t}) < \infty$. For each $k = 1, \dots, K$, score function $u_{\rho,k,t}$, asymptotically at the true values of parameters, is white noise, because $u_{\rho,k,t}$, asymptotically, is a MDS and $\text{Var}(u_{\rho,k,t}) < \infty$. Hence, if $|\phi| < 1$, $|\beta| < 1$, and $|\gamma_k| < 1$, then, asymptotically at the true values of parameters, μ_t, λ_t, and $\rho_{k,t}$ are covariance stationary and are $\mathcal{F}$-measurable functions of ϵ_s for all $s < t$.

2.5 MC simulation experiments

For all MC experiments, zero mean $\mu_t = 0$, unit scale $\exp(\lambda_t) = 1$, and score-driven shape parameters are used for $t = 1, \dots, T$. Two sets of true parameter values are used: The first set assumes high persistence for the shape parameters (i.e. $\gamma_k = 0.95$ for all k). The second set assumes low persistence for the shape parameters

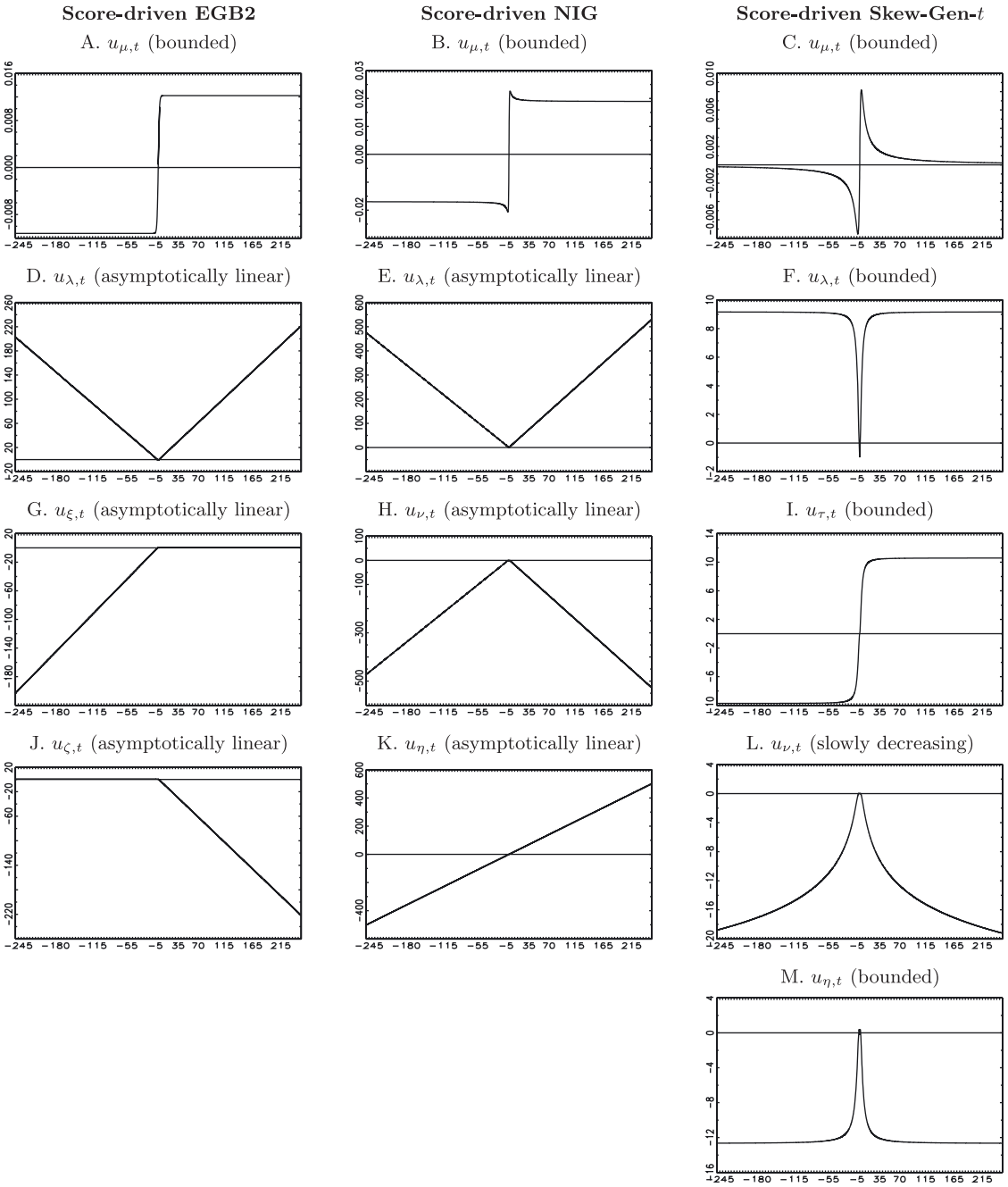

Figure 2: Score functions for models with score-driven location, scale, and shape parameters. The score functions are presented as a function of $\epsilon_t \in [-250, 250]$, to show the asymptotic properties of the score functions for $|\epsilon_t| \to \infty$. In the score functions the dynamic parameters are replaced by their unconditional means.

(i.e. $\gamma_k = 0.15$ for all k). The true values of all parameters are presented in Table 1. By using those true values, 1,000 trajectories are simulated, and each trajectory includes $T = 10,000$ periods. By using the ML method, the parameters of the score-driven models with dynamic shape parameters are estimated for each trajectory.

We study the parameter estimates by using non-parametric methods. In Table 1, the 5, 50, and 95% quantiles of the 1,000 parameter estimates are reported. For the high-persistence case, the medians give a

Table 1: Monte Carlo simulation experiments.

	True values #1	5% quantile	Median	95% quantile	True values #2	5% quantile	Median	95% quantile
				A. Score-driven EGB2				
δ_1	−0.0500	−0.0721	−0.0526	−0.0375	−0.0500	−0.1045	−0.0753	−0.0413
γ_1	0.9500	0.9307	0.9490	0.9636	0.1500	0.0004	0.1509	0.5167
κ_1	0.0500	0.0399	0.0498	0.0606	0.0500	0.0331	0.0504	0.0686
δ_2	−0.0500	−0.0596	−0.0501	−0.0415	−0.0500	−0.0468	−0.0251	−0.0065
γ_2	0.9500	0.9407	0.9500	0.9583	0.1500	0.0002	0.1529	0.5239
κ_2	−0.0500	−0.0582	−0.0500	−0.0424	−0.0500	−0.0678	−0.0494	−0.0304
				B. Score-driven NIG				
δ_1	0.0500	0.0290	0.0616	0.1287	0.0500	0.0146	0.0642	0.1051
γ_1	0.9500	0.8917	0.9479	0.9754	0.1500	0.0007	0.1495	0.7644
κ_1	0.0500	0.0263	0.0445	0.0673	0.0500	0.0001	0.0481	0.1193
δ_2	−0.0500	−0.0837	−0.0674	−0.0541	−0.0500	−0.1750	−0.1406	−0.0918
γ_2	0.9500	0.9284	0.9420	0.9534	0.1500	0.0002	0.1445	0.4403
κ_2	0.0500	0.0399	0.0452	0.0509	0.0500	0.0328	0.0487	0.0647
				C. Score-driven Skew-Gen-*t*				
δ_1	−0.0200	−0.0352	−0.0294	−0.0133	−0.04	−0.1057	−0.0859	−0.0669
γ_1	0.9500	0.9394	0.9489	0.9587	0.15	0.0002	0.1511	0.3201
κ_1	0.0500	0.0445	0.0485	0.0542	0.05	0.0405	0.0494	0.0580
δ_2	0.0800	0.0367	0.0729	0.2177	1.3	0.5043	1.0005	1.4774
γ_2	0.9500	0.9466	0.9495	0.9854	0.15	0.1061	0.1382	0.1524
κ_2	0.0500	0.0479	0.0501	0.2987	0.05	0.0404	0.0497	0.0591
δ_3	0.0300	0.0180	0.0317	0.0709	0.05	0.0175	0.0828	0.1621
γ_3	0.9500	0.9082	0.9492	0.9765	0.15	0.0005	0.1504	0.6737
κ_3	0.0500	0.0319	0.0501	0.0782	0.05	0.0040	0.0512	0.0981

Exponential generalized beta distribution of the second kind (EGB2); normal-inverse Gaussian (NIG) distribution; skewed generalized *t*-distribution (Skew-Gen-*t*). Number of simulated trajectories: 1,000; sample size: $T = 10{,}000$. For all models, $\mu_t = 0$ and $\exp(\lambda_t) = 1$ for $t = 1, \ldots, T$. True values #1 imply high persistence for the shape parameters. True values #2 imply low persistence for the shape parameters. The data generating processes are given by: For the score-driven EGB2 model, $y_t \sim$ EGB2 $[0, 1, \exp(\xi_t), \exp(\zeta_t)]$, where $\xi_t = \delta_1 + \gamma_1 \xi_{t-1} + \kappa_1 u_{\xi,t-1}$ and $\zeta_t = \delta_2 + \gamma_2 \zeta_{t-1} + \kappa_2 u_{\zeta,t-1}$. For the score-driven NIG model, $y_t \sim$ NIG$[0, 1, \exp(\nu_t), \exp(\nu_t)\ \tanh(\eta_t)]$, where $\nu_t = \delta_1 + \gamma_1 \nu_{t-1} + \kappa_1 u_{\nu,t-1}$ and $\eta_t = \delta_2 + \gamma_2 \eta_{t-1} + \kappa_2 u_{\eta,t-1}$. For the score-driven Skew-Gen-*t* model, $\epsilon_t \sim$ Skew-Gen-*t*$[0, 1, \tanh(\tau_t), \exp(\nu_t) + 4, \exp(\eta_t)]$, where $\tau_t = \delta_1 + \gamma_1 \tau_{t-1} + \kappa_1 u_{\tau,t-1}$, $\nu_t = \delta_1 + \gamma_1 \nu_{t-1} + \kappa_1 u_{\nu,t-1}$, and $\eta_t = \delta_2 + \gamma_2 \eta_{t-1} + \kappa_2 u_{\eta,t-1}$. For the initial condition, the unconditional mean of each dynamic shape parameter is used.

good approximation of the true values, and the 90% confidence intervals of the quantiles include all true values. For the low-persistence case, the medians give a good approximation of the majority of the true values; the only exceptions are some of the constant parameters, for which the true value is not within the 90% confidence interval (i.e. δ_2 for the EGB2 and NIG models). For the score-driven Skew-Gen-*t* model, for all parameters, the true value is within the 90% confidence interval for both the high- and low-persistence cases. The medians indicate that γ_k and κ_k are consistently estimated for all cases, supporting the use of the score-driven Skew-Gen-*t* model.

3 Control data

Daily data are used from the opening and closing prices of the S&P 500 index, p_{t-1} and p_t, respectively, for trading day t for the period of February 14, 1990 to October 21, 2021 (source of data: Bloomberg). Daily data of the 5 min realized volatility of the S&P 500 are obtained from the Oxford Man Institute of Quantitative

Table 2: Descriptive statistics for daily log-returns on the S&P 500 index, $y_t = \ln(p_t/p_{t-1})$.

	Full sample period	RV sample period	dot.com boom	2008 US Financial Crisis	COVID-19 pandemic
Start date	February 14, 1990	January 3, 2000	January 2, 1997	October 1, 2007	January 9, 2020
End date	October 21, 2021	October 21, 2021	October 9, 2002	March 31, 2009	October 21, 2021
Sample size T	7984	5487	1452	378	451
Minimum	−0.1277	−0.1277	−0.0711	−0.0947	−0.1277
Maximum	0.1096	0.1096	0.0557	0.1096	0.0897
Mean	0.0003	0.0002	0.0000	−0.0017	0.0007
Standard deviation	0.0114	0.0124	0.0133	0.0242	0.0172
Skewness	−0.4146	−0.3993	−0.1129	0.0068	− 1.0344
Excess kurtosis	11.4290	11.0638	2.2434	3.6156	13.9885
Corr (y_t, y_{t-1})	−0.0870	−0.1120	−0.0009	−0.1552	−0.3188
Corr$\left(y_t^2, y_{t-1}\right)$	−0.1035	−0.1035	−0.1453	−0.1274	−0.0802

Realized volatility (RV); United States (US); coronavirus disease (COVID-19); correlat). *Source of data*: Bloomberg.

Finance (https://www.oxford-man.ox.ac.uk/resources/the-realized-library/) for the period of January 3, 2000 to October 21, 2021. The 5 min realized volatility is estimated by using data when the markets are open. This motivates the use of the log-percentage change between the opening and closing prices for each trading day. In Table 2, descriptive statistics of daily log-returns on the S&P 500, $y_t = \ln(p_t/p_{t-1})$ for $t = 1, \dots, T$ (pre-sample data are used for p_0), for the full sample and the realized volatility periods, are presented. In addition, in Table 2, we also present the descriptive statistics of y_t for the dot.com boom, 2008 US Financial Crisis, and COVID-19 pandemic subperiods, for which VaR backtesting is performed.

The positive excess kurtosis estimates suggests heavy tails of y_t. The negative correlation coefficient Corr$\left(y_t^2, y_{t-1}\right)$ suggests that high volatility often follows significant negative returns, which motivates the consideration of leverage effects within λ_t. The evolution of y_t is presented in Panel A of Figure 3, where extreme observations are indicated by using the $\overline{\mu} \pm 4\overline{\sigma}$ interval; $\overline{\mu}$ and $\overline{\sigma}$ are the sample estimates of mean and standard deviation, respectively. In Panel B of Figure 3, the high number of outliers during the dot.com boom, 2008 US Financial Crisis, and COVID-19 pandemic subperiods are indicated. Finally, in Panel C of Figure 3, the conditional volatility estimates for S&P 500 returns for one of the best-performing volatility models of the present paper are shown.

4 Method implementation and results

4.1 In-sample estimation and forecasting

The in-sample parameter estimates for all models for the period of February 14, 1990 to October 21, 2021 are presented in Tables C1–C4 of Appendix C. The in-sample parameter estimates for all models for the period of January 3, 2000 to October 21, 2021 are presented in Tables 3–6. For most of the specifications the ϕ and θ parameters which measure the expected return dynamics, are significantly different from zero. For all specifications, highly significant ω, α, α^*, and β parameters are found for the scale. For most of the specifications, the dynamic parameters of shape (i.e. γ_1, γ_2, and γ_3), and the scaling parameter of the score function with respect to shape (i.e. κ_1, κ_2, and κ_3) are significant. All estimates of ϕ, β, γ_1, γ_2, and γ_3 are less than one in absolute value.

Moreover, we also report specification and statistical performance test results in Tables 3–6 and C1–C4. (i) For most of the specifications, the MDS null hypothesis of the Escanciano–Lobato test is not rejected up to the fourth moment, which supports the correct the model specification assumption (S1). (ii) In-sample statistical performances are compared by using the LR test. For many cases, we find that the performance

A. S&P 500 log-returns y_t. The horizontal lines show $\overline{\mu} \pm 4\overline{\sigma}$, respectively.

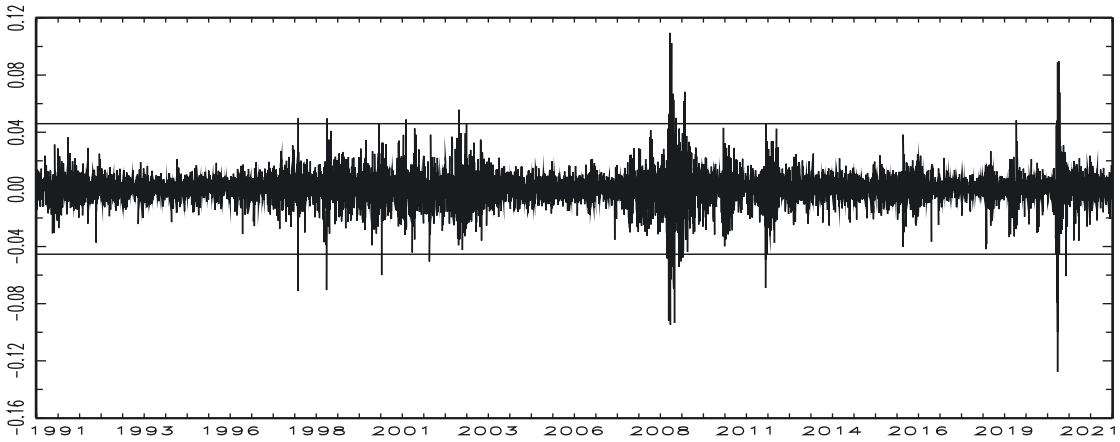

B. News arrival times of those S&P 500 log-returns, which are outside the interval $\overline{\mu} \pm 4\overline{\sigma}$

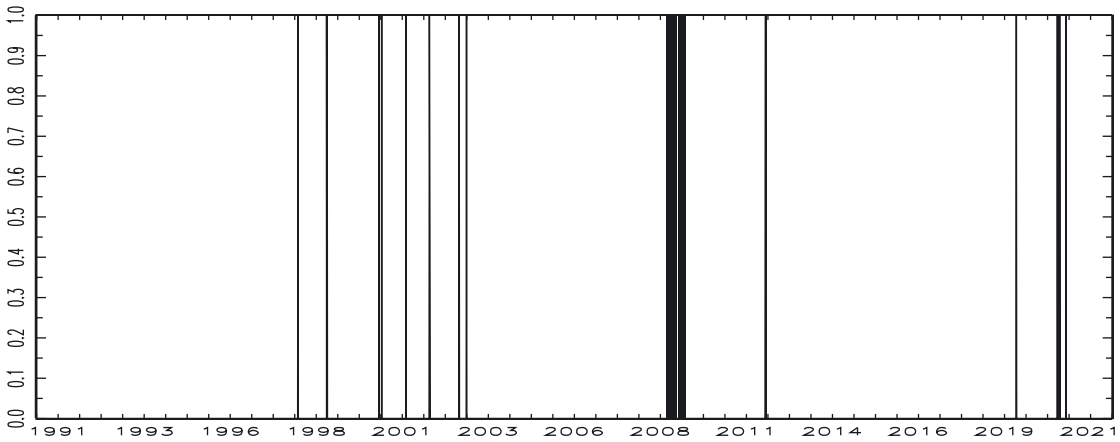

C. Volatility estimates for the score-driven Skew-Gen-t model with dynamic shape parameters τ_t, ν_t, and η_t

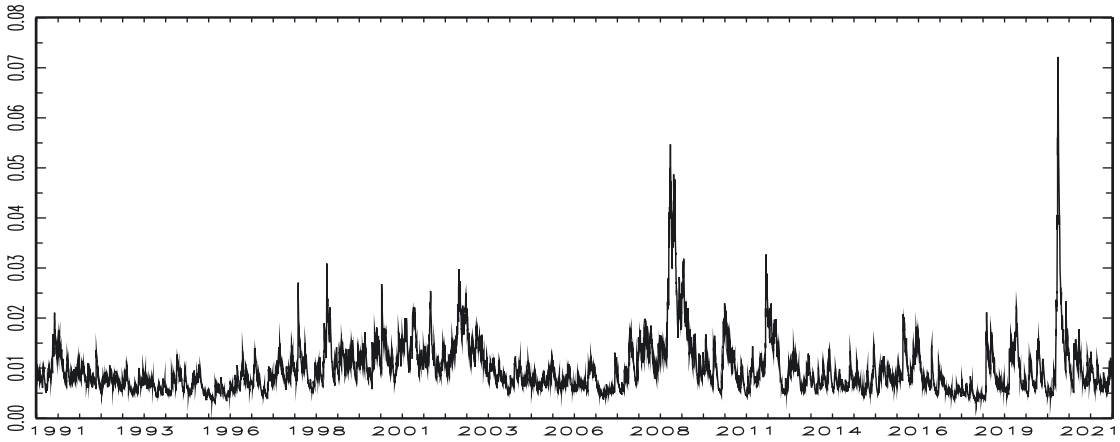

Figure 3: S&P 500 log-returns y_t, outliers, and volatility estimates for the period of February 14, 1990 to October 21, 2021. $\overline{\mu}$ and $\overline{\sigma}$ are the sample estimates of mean and standard deviation, respectively, of y_t. The parameter estimates for the score-driven Skew-Gen-t model are presented in Table C3 of Appendix C. During the sample period of 7,984 trading days there are 54 outliers, which are defined according to the $\overline{\mu} \pm 4\overline{\sigma}$ criterion.

Table 3: ML estimates for the score-driven EGB2 models for the period of January 3, 2000 to October 21, 2021.

Constant ξ_t and ζ_t		Dynamic ξ_t and ζ_t		Dynamic ξ_t and constant ζ_t		Constant ξ_t and dynamic ζ_t	
c	0.0009*** (0.0003)	C	0.0015 (0.0036)	C	0.0009*** (0.0003)	C	0.0015 (0.0119)
ϕ	0.3548** (0.1715)	Φ	−0.1452 (2.6953)	Φ	0.3755** (0.1790)	Φ	−0.0716 (8.7600)
θ	−0.0503*** (0.0114)	Θ	−0.0044 (0.0182)	Θ	−0.0567*** (0.0136)	Θ	−0.0006 (0.0160)
ω	−0.0757*** (0.0153)	Ω	−0.0696*** (0.0147)	ω	−0.0709*** (0.0149)	Ω	−0.0722*** (0.0149)
α	0.0453*** (0.0043)	α	0.0474*** (0.0042)	α	0.0445*** (0.0043)	α	0.0477*** (0.0042)
α^*	0.0489*** (0.0032)	α^*	0.0458*** (0.0034)	α^*	0.0480*** (0.0034)	α^*	0.0464*** (0.0032)
β	0.9876*** (0.0027)	β	0.9886*** (0.0026)	β	0.9884*** (0.0027)	β	0.9882*** (0.0027)
λ_0	−5.0013*** (0.3686)	λ_0	−5.0315*** (0.3765)	λ_0	−4.9972*** (0.3676)	λ_0	−5.0347*** (0.4521)
δ_1	−0.5241*** (0.1120)	δ_1	−0.2604 (0.5204)	δ_1	−0.2753 (0.3492)	δ_1	−0.5439*** (0.1111)
		γ_1	0.5143 (0.9635)	γ_1	0.4623 (0.6688)		
		κ_1	0.0090 (0.0152)	κ_1	0.0153 (0.0151)		
δ_2	−0.3471*** (0.1206)	δ_2	−0.1889** (0.0772)	δ_2	−0.3383*** (0.1208)	δ_2	−0.1996** (0.0779)
		γ_2	0.4727*** (0.1220)			γ_2	0.4516*** (0.1187)
		κ_2	−0.1150*** (0.0292)			κ_2	−0.1162*** (0.0286)
MDS (mean)	0.2366 (0.6267)	MDS (mean)	0.1390 (0.7093)	MDS (mean)	0.7689 (0.3806)	MDS (mean)	0.3716 (0.5421)
MDS (variance)	0.2871 (0.5921)	MDS (variance)	0.3235 (0.5695)	MDS (variance)	0.2127 (0.6447)	MDS (variance)	0.3651 (0.5457)
MDS (skewness)	0.8160 (0.3663)	MDS (skewness)	0.2213 (0.6380)	MDS (skewness)	2.9030 (0.0884)	MDS (skewness)	0.0011 (0.9731)
MDS (kurtosis)	0.9958 (0.3183)	MDS (kurtosis)	0.9033 (0.3419)	MDS (kurtosis)	0.0004 (0.9848)	MDS (kurtosis)	1.5504 (0.2131)
LL	3.2801	LL	3.2824	LL	3.2802	LL	3.2823
LR	24.3436 (0.0001)	LR	NA	LR	23.3230 (0.0000)	LR	0.4247 (0.8087)
RMSE for RV	0.004038	RMSE for RV	0.004044 (0.7529)	RMSE for RV	0.004031 (0.6255)	RMSE for RV	0.004042 (0.7388)
MAE for RV	0.003003	MAE for RV	0.002998 (0.6486)	MAE for RV	0.003000 (0.6937)	MAE for RV	0.002999 (0.5099)

Exponential generalized beta distribution of the second kind (EGB2); martingale difference sequence (MDS); log-likelihood (LL); likelihood-ratio (LR); not available (NA); realized volatility (RV); root mean squared error (RMSE); mean absolute error (MAE). ** and *** indicate significance at the 5 and 1% levels, respectively. For the parameter estimates standard errors are reported in parentheses. For all other statistics of the table, *p*-values are reported in parentheses. The null hypothesis of the MDS test is the correctness of the EGB2 specification, which is checked up to the first four conditional moments. For the LR test, the most general model is the score-driven model for which all shape parameters are time-varying; the rest of the specifications are special cases, so the classical LR test can be used. The SE and AE loss functions compare the in-sample volatility forecasting accuracy with respect to the 5 min RV. The volatility forecasting accuracy of the score-driven model with constant shape parameters is compared with the volatility forecasting accuracies of thescore-driven models with time-varying shape parameters, by using the OLS-HAC (ordinary least squares, heteroskedasticity and autocorrelation consistent) estimator of a linear regression of the difference of the loss functions of the competing models on a constant parameter. The *p*-value for the significance of the constant parameter is reported for the RMSE and MAE statistics. Model specification: $y_t = \mu_t + \exp(\lambda_t)\,\epsilon_t$, $\epsilon_t \sim$EGB2 [0, 1, $\exp(\xi_t)$, $\exp(\zeta_t)$], $\mu_t = c + \phi\mu_{t-1} + \theta u_{\mu,t-1}$, and $\lambda_t = \omega + \beta\lambda_{t-1} + \alpha u_{\lambda,t-1} + \alpha^* \operatorname{sgn}(-\epsilon_{t-1})\,(u_{\lambda,t-1} + 1)$. For constant ξ_t or ζ_t: $\xi_t = \delta_1$ and $\zeta_t = \delta_2$. For dynamic ξ_t or ζ_t: $\xi_t = \delta_1 + \gamma_1\xi_{t-1} + \kappa_1 u_{\xi,t-1}$ and $\zeta_t = \delta_2 + \gamma_2\zeta_{t-1} + \kappa_2 u_{\zeta,t-1}$.

Table 4: Parameter estimates for the score-driven NIG models for the period of January 3, 2000 to October 21, 2021.

Constant ν_t and η_t		Dynamic ν_t and η_t		Dynamic ν_t and constant η_t		Constant ν_t and dynamic η_t	
c	0.0009*** (0.0003)	C	0.0011*** (0.0004)	c	0.0009*** (0.0003)	C	0.0009* (0.0005)
ϕ	0.3478** (0.1767)	Φ	0.2114 (0.2757)	ϕ	0.3535** (0.1722)	Φ	0.3703 (0.3196)
θ	−0.0303*** (0.0073)	Θ	−0.0259*** (0.0085)	θ	−0.0309*** (0.0073)	Θ	−0.0253** (0.0108)
ω	−0.0624*** (0.0122)	Ω	−0.0718*** (0.0129)	ω	−0.0662*** (0.0126)	Ω	−0.0631*** (0.0122)
α	0.0463*** (0.0043)	α	0.0490*** (0.0047)	α	0.0476*** (0.0046)	α	0.0462*** (0.0043)
α^*	0.0501*** (0.0034)	α^*	0.0495*** (0.0036)	α^*	0.0496*** (0.0034)	α^*	0.0504*** (0.0037)
β	0.9874*** (0.0028)	β	0.9853*** (0.0029)	β	0.9865*** (0.0029)	β	0.9872*** (0.0028)
λ_0	−3.8244*** (0.3557)	λ_0	−3.8101*** (0.3612)	λ_0	−3.8109*** (0.3593)	λ_0	−3.8232*** (0.3550)
δ_1	0.5062*** (0.1002)	δ_1	0.8712*** (0.2178)	δ_1	0.8338*** (0.2308)	δ_1	0.5029*** (0.1001)
		γ_1	−0.7121*** (0.2106)	γ_1	−0.6452** (0.2662)		
		κ_1	−0.0622* (0.0324)	κ_1	−0.0654** (0.0332)		
δ_2	−0.1124*** (0.0192)	δ_2	−0.0165 (0.0155)	δ_2	−0.1107*** (0.0193)	δ_2	−0.0862 (0.1528)
		γ_2	0.8535*** (0.1367)			γ_2	0.2382 (1.3655)
		κ_2	−0.0087 (0.0069)			κ_2	−0.0079 (0.0119)
MDS (mean)	0.3221 (0.5703)	MDS (mean)	0.0260 (0.8720)	MDS (mean)	0.3100 (0.5777)	MDS (mean)	0.0459 (0.8304)
MDS (variance)	0.3555 (0.5510)	MDS (variance)	0.8255 (0.3636)	MDS (variance)	0.9114 (0.3397)	MDS (variance)	0.3642 (0.5462)
MDS (skewness)	0.8359 (0.3606)	MDS (skewness)	0.6901 (0.4061)	MDS (skewness)	0.8457 (0.3578)	MDS (skewness)	0.7022 (0.4021)
MDS (kurtosis)	0.9995 (0.3174)	MDS (kurtosis)	1.1170 (0.2906)	MDS (kurtosis)	1.0728 (0.3003)	MDS (kurtosis)	1.0252 (0.3113)
LL	3.2804	LL	3.2811	LL	3.2809	LL	3.2805
LR	7.7992 (0.0992)	LR	NA	LR	3.0365 (0.2191)	LR	7.3548 (0.0253)
RMSE for RV	0.004046	RMSE for RV	0.004052 (0.6751)	RMSE for RV	0.004048 (0.8461)	RMSE for RV	0.004048 (0.5317)
MAE for RV	0.003012	MAE for RV	0.003006 (0.4114)	MAE for RV	0.003007 (0.3942)	MAE for RV	0.003012 (0.9020)

Normal-inverse Gaussian (NIG) distribution; martingale difference sequence (MDS); log-likelihood (LL); likelihood-ratio (LR); not available (NA); realized volatility (RV); root mean squared error (RMSE); mean absolute error (MAE). *, **, and *** indicate significance at the 10, 5, and 1% levels, respectively. For the parameter estimates standard errors are reported in parentheses. For all other statistics of the table, p-values are reported in parentheses. The null hypothesis of the MDS test is the correctness of the NIG specification, which is checked up to the first four conditional moments. For the LR test, the most general model is the score-driven model for which all shape parameters are time-varying; the rest of the specifications are special cases, so the classical LR test can be used. The SE and AE loss functions compare the in-sample volatility forecasting accuracy with respect to the 5 min RV. The volatility forecasting accuracy of the score-driven model with constant shape parameters is compared with the volatility forecasting accuracies of the score-driven models with time-varying shape parameters, by using the OLS-HAC (ordinary least squares, heteroskedasticity and autocorrelation consistent) estimator of a linear regression of the difference of the loss functions of the competing models on a constant parameter. The p-value for the significance of the constant parameter is reported for the RMSE and MAE statistics. Model specification: $y_t = \mu_t + \exp(\lambda_t)\,\epsilon_t$, $\epsilon_t \sim$NIG [0, 1, $\exp(\nu_t)$, $\exp(\nu_t)\,\tanh(\eta_t)$], $\mu_t = c + \phi\mu_{t-1} + \theta u_{\mu,t-1}$, and $\lambda_t = \omega + \beta\lambda_{t-1} + \alpha u_{\lambda,t-1} + \alpha^*\,\mathrm{sgn}(-\epsilon_{t-1})\,(u_{\lambda,t-1} + 1)$. For constant ν_t or η_t: $\nu_t = \delta_1$ and $\eta_t = \delta_2$. For dynamic ν_t or η_t: $\nu_t = \delta_1 + \gamma_1\nu_{t-1} + \kappa_1 u_{\nu,t-1}$ and $\eta_t = \delta_2 + \gamma_2\eta_{t-1} + \kappa_2 u_{\eta,t-1}$.

Table 5: Parameter estimates for the score-driven Skew-Gen-t models for the period of January 3, 2000 to October 21, 2021.

Constant τ_t, ν_t and η_t		Dynamic τ_t, ν_t and η_t		Dynamic τ_t, ν_t and constant η_t		Dynamic τ_t, constant ν_t and dynamic η_t	
c	0.0009^{***} (0.0002)	C	0.0010^{***} (0.0003)	c	0.0010^{***} (0.0003)	c	0.0010^{***} (0.0003)
ϕ	0.3471^{**} (0.1611)	Φ	0.2525 (0.1947)	ϕ	0.2448 (0.2299)	Φ	0.2577 (0.2239)
θ	-0.0863^{***} (0.0180)	Θ	-0.0802^{***} (0.0205)	θ	-0.0745^{***} (0.0226)	Θ	-0.0758^{***} (0.0224)
ω	-0.0705^{***} (0.0131)	Ω	-0.0765^{***} (0.0123)	ω	-0.0702^{***} (0.0131)	Ω	-0.0713^{***} (0.0133)
α	0.0470^{***} (0.0042)	α	0.0471^{***} (0.0042)	α	0.0472^{***} (0.0043)	α	0.0474^{***} (0.0044)
α^*	0.0490^{***} (0.0033)	α^*	0.0456^{***} (0.0033)	α^*	0.0484^{***} (0.0035)	α^*	0.0482^{***} (0.0035)
β	0.9865^{***} (0.0027)	β	0.9853^{***} (0.0025)	β	0.9866^{***} (0.0027)	β	0.9863^{***} (0.0027)
λ_0	-4.2375^{***} (0.3547)	λ_0	-4.2208^{***} (0.3574)	λ_0	-4.2357^{***} (0.3543)	λ_0	-4.2388^{***} (0.3535)
δ_1	-0.0890^{***} (0.0148)	δ_1	−0.0237 (0.0260)	δ_1	−0.0248 (0.0267)	δ_1	−0.0237 (0.0268)
		γ_1	0.7374^{**} (0.2871)	γ_1	0.7284^{**} (0.2899)	γ_1	0.7382^{**} (0.2942)
		κ_1	−0.0064 (0.0065)	κ_1	−0.0069 (0.0071)	κ_1	−0.0065 (0.0067)
δ_2	2.0371^{***} (0.3145)	δ_2	0.5727 (0.4676)	δ_2	1.8789 (1.5438)	δ_2	2.0453^{***} (0.3527)
		γ_2	0.7858^{***} (0.1731)	γ_2	0.1022 (0.7006)		
		κ_2	2.2455 (1.5656)	κ_2	1.4535 + (0.8896)		
δ_3	0.4827^{***} (0.0501)	δ_3	0.0207^{*} (0.0111)	δ_3	0.4725^{***} (0.0549)	δ_3	0.2144 (1.4936)
		γ_3	0.9513^{***} (0.0255)			γ_3	0.5514 (3.1260)
		κ_3	-0.0405^{**} (0.0203)			κ_3	0.0051 (0.0205)
MDS (mean)	0.0438 (0.8342)	MDS (mean)	0.4988 (0.4800)	MDS (mean)	0.1622 (0.6872)	MDS (mean)	0.1031 (0.7481)
MDS (variance)	0.2588 (0.6109)	MDS (variance)	0.0253(0.8736)	MDS (variance)	0.0143 (0.9047)	MDS (variance)	0.1837 (0.6682)
MDS (skewness)	0.8958 (0.3439)	MDS (skewness)	0.6877 (0.4070)	MDS (skewness)	0.7747 (0.3788)	MDS (skewness)	0.6504 (0.4200)
MDS (kurtosis)	0.9412 (0.3320)	MDS (kurtosis)	0.8992 (0.3430)	MDS (kurtosis)	1.0198 (0.3126)	MDS (kurtosis)	0.8890 (0.3458)
LL	3.2824	LL	3.2834	LL	3.2826	LL	3.2825
LR	10.7787 (0.0955)	LR	NA	LR	8.0088 (0.0182)	LR	9.1402 (0.0104)
RMSE for RV	0.004019	RMSE for RV	0.003962^{***} (0.0025)	RMSE for RV	0.004018 (0.9412)	RMSE for RV	0.004021 (0.5675)
MAE for RV	0.002980	MAE for RV	0.002938^{***} (0.0000)	MAE for RV	0.002980 (0.9224)	MAE for RV	0.002981 (0.6438)

Skewed generalized t-distribution (Skew-Gen-t); martingale difference sequence (MDS); log-likelihood (LL); likelihood-ratio (LR); not available (NA); realized volatility (RV); root mean squared error (RMSE); mean absolute error (MAE). +, *, **, and *** indicate significance at the 15, 10, 5, and 1% levels, respectively. For the parameter estimates standard errors are reported in parentheses. For all other statistics of the table, p-values are reported in parentheses. The null hypothesis of the MDS test is the correctness of the Skew-Gen-t specification, which is checked up to the first four conditional moments. For the LR test, the most general model is the score-driven model for which all shape parameters are time-varying; the rest of the specifications are special cases, so the classical LR test can be used. The SE and AE loss functions compare the in-sample volatility forecasting accuracy with respect to the 5 min RV. The volatility forecasting accuracy of the score-driven model with constant shape parameters is compared with the volatility forecasting accuracies of the score-driven models with time-varying shape parameters, by using the OLS-HAC (ordinary least squares, heteroskedasticity and autocorrelation consistent) estimator of a linear regression of the difference of the loss functions of the competing models on a constant parameter. The p-value for the significance of the constant parameter is reported for the RMSE and MAE statistics. Model specification: $y_t = \mu_t + \exp(\lambda_t)\,\epsilon_t$, $\epsilon_t \sim$ Skew-Gen-$t[0, 1, \tanh(\tau_t), \exp(\nu_t)+4, \exp(\eta_t)]$, $\mu_t = c + \phi\mu_{t-1} + \theta u_{\mu,t-1}$, and $\lambda_t = \omega + \beta\lambda_{t-1} + \alpha u_{\lambda,t-1} + \alpha^* \operatorname{sgn}(-\epsilon_{t-1})\,(u_{\lambda,t-1}+1)$. For constant τ_t, ν_t, or η_t: $\tau_t = \delta_1$, $\nu_t = \delta_2$, and $\eta_t = \delta_3$. For dynamic τ_t, ν_t, or η_t: $\tau_t = \delta_1 + \gamma_1\tau_{t-1} + \kappa_1 u_{\tau,t-1}$, $\nu_t = \delta_2 + \gamma_2\nu_{t-1} + \kappa_2 u_{\nu,t-1}$, and $\eta_t = \delta_3 + \gamma_3\eta_{t-1} + \kappa_3 u_{\eta,t-1}$.

Table 6: Parameter estimates for the score-driven Skew-Gen-t models for the period of January 3, 2000 to October 21, 2021.

Dynamic τ_t and constant ν_t, η_t		Constant τ_t and dynamic ν_t, η_t		Constant τ_t, dynamic ν_t and constant η_t		Constant τ_t, ν_t and dynamic η_t	
c	0.0010^{***} (0.0003)	C	0.0009^{***} (0.0002)	C	0.0009^{***} (0.0002)	C	0.0009^{***} (0.0002)
ϕ	0.2429 (0.2273)	Φ	0.3571^{**} (0.1438)	Φ	0.2975^{*} (0.1678)	Φ	0.3481^{**} (0.1614)
θ	-0.0754^{***} (0.0224)	Θ	-0.0890^{***} (0.0168)	Θ	-0.0875^{***} (0.0181)	Θ	-0.0860^{***} (0.0180)
ω	-0.0718^{***} (0.0132)	Ω	-0.0753^{***} (0.0122)	ω	-0.0695^{***} (0.0131)	Ω	-0.0706^{***} (0.0132)
α	0.0475^{***} (0.0042)	α	0.0466^{***} (0.0041)	α	0.0467^{***} (0.0042)	α	0.0470^{***} (0.0044)
α^*	0.0483^{***} (0.0034)	α^*	0.0462^{***} (0.0033)	α^*	0.0494^{***} (0.0035)	α^*	0.0490^{***} (0.0034)
β	0.9863^{***} (0.0027)	β	0.9856^{***} (0.0025)	β	0.9867^{***} (0.0027)	β	0.9865^{***} (0.0027)
λ_0	-4.2364^{***} (0.3551)	λ_0	-4.2179^{***} (0.3573)	λ_0	-4.2342^{***} (0.3555)	λ_0	-4.2373^{***} (0.3549)
δ_1	−0.0243 (0.0266)	δ_1	-0.0882^{***} (0.0140)	δ_1	-0.0894^{***} (0.0148)	δ_1	-0.0891^{***} (0.0148)
γ_1	0.7342^{**} (0.2888)						
κ_1	−0.0066 (0.0066)						
δ_2	2.0439^{***} (0.3402)	δ_2	0.5957 (0.5114)	δ_2	2.0828 (1.4554)	δ_2	2.0362^{***} (0.3311)
		γ_2	0.7743^{***} (0.1913)	γ_2	0.0077 (0.6529)		
		κ_2	2.0571 + (1.3994)	κ_2	1.4402^{*} (0.8341)		
δ_3	0.4783^{***} (0.0531)	δ_3	0.0210^{*} (0.0109)	δ_3	0.4745^{***} (0.0536)	δ_3	0.1998(6.3700)
		γ_3	0.9513^{***} (0.0247)			γ_3	0.5863(13.1865)
		κ_3	-0.0410^{**} (0.0199)			κ_3	−0.0011(0.0210)
MDS (mean)	0.0992 (0.7529)	MDS (mean)	0.0157 (0.9002)	MDS (mean)	0.0067 (0.9346)	MDS (mean)	0.0494 (0.8241)
MDS (variance)	0.2121 (0.6452)	MDS (variance)	0.0528 (0.8183)	MDS (variance)	0.0444 (0.8331)	MDS (variance)	0.2649 (0.6068)
MDS (skewness)	0.6551 (0.4183)	MDS (skewness)	0.9253 (0.3361)	MDS (skewness)	1.2069 (0.2719)	MDS (skewness)	0.8952 (0.3441)
MDS (kurtosis)	0.9820 (0.3217)	MDS (kurtosis)	0.8159 (0.3664)	MDS (kurtosis)	0.9683 (0.3251)	MDS (kurtosis)	0.9579 (0.3277)
LL	3.2825	LL	3.2832	LL	3.2825	LL	3.2824
LR	9.1808 (0.0567)	LR	1.6033 (0.4486)	LR	9.8228 (0.0435)	LR	10.7765 (0.0292)
RMSE for RV	0.004020 (0.6882)	RMSE for RV	0.003958^{***} (0.0002)	RMSE for RV	0.004014 (0.2897)	RMSE for RV	0.004019 (0.9227)
MAE for RV	0.002981 (0.6716)	MAE for RV	0.002936^{***} (0.0000)	MAE for RV	0.002981 (0.6727)	MAE for RV	0.002980 (0.8936)

Skewed generalized t-distribution (Skew-Gen-t); martingale difference sequence (MDS); log-likelihood (LL); likelihood-ratio (LR); not available (NA); realized volatility (RV); root mean squared error (RMSE); mean absolute error (MAE). +, *, **, and ***indicate significance at the 15, 10, 5, and 1% levels, respectively. For the parameter estimates standard errors are reported in parentheses. For all other statistics of the table, p-values are reported in parentheses. The null hypothesis of the MDS test is the correctness of the Skew-Gen-t specification, which is checked up to the first four conditional moments. For the LR test, the most general model is the score-driven model for which all shape parameters are time-varying; the rest of the specifications are special cases, so the classical LR test can be used. The SE and AE loss functions compare the in-sample volatility forecasting accuracy with respect to the 5 min RV. The volatility forecasting accuracy of the score-driven model with constant shape parameters is compared with the volatility forecasting accuracies of the score-driven models with time-varying shape parameters, by using the OLS-HAC (ordinary least squares, heteroskedasticity and autocorrelation consistent) estimator of a linear regression of the difference of the loss functions of the competing models on a constant parameter. The p-value for the significance of the constant parameter is reported for the RMSE and MAE statistics. Model specification: $y_t = \mu_t + \exp(\lambda_t)\,\epsilon_t$, $\epsilon_t \sim$Skew-Gen-$t[0, 1, \tanh(\tau_t), \exp(\nu_t) + 4, \exp(\eta_t)]$, $\mu_t = c + \phi\mu_{t-1} + \theta u_{\mu,t-1}$, and $\lambda_t = \omega + \beta\lambda_{t-1} + \alpha u_{\lambda,t-1} + \alpha^* \operatorname{sgn}(-\epsilon_{t-1})\,(u_{\lambda,t-1} + 1)$. For constant τ_t, ν_t, or η_t: $\tau_t = \delta_1$, $\nu_t = \delta_2$, and $\eta_t = \delta_3$. For dynamic τ_t, ν_t, or η_t: $\tau_t = \delta_1 + \gamma_1\tau_{t-1} + \kappa_1 u_{\tau,t-1}$, $\nu_t = \delta_2 + \gamma_2\nu_{t-1} + \kappa_2 u_{\nu,t-1}$, and $\eta_t = \delta_3 + \gamma_3\eta_{t-1} + \kappa_3 u_{\eta,t-1}$.

of the score-driven specifications with dynamic shape parameters are superior to the performance of the score-driven model with constant shape parameters.

For the most general score-driven Skew-Gen-t model of this paper, the evolution of the shape parameters $\tanh(\tau_t)$, $\exp(\nu_t)+4$, and $\exp(\eta_t)$, and the evolution of the scale parameter $\exp(\lambda_t)$ are presented in Figure 4. The lowest values of $\exp(\nu_t)+4$ indicate the extreme events which significantly impacted the US stock market, and the circumstances of those events are described in Appendix D.

In Tables 3–6, we also report in-sample volatility forecasting accuracy test results. As aforementioned, we use the 5 min realized volatility σ_t^* as a proxy of true volatility (Liu, Patton, and Sheppard 2015; Harvey and Lange 2018). The estimated conditional volatility for each model is denoted $\sigma(y_t|\mathcal{F}_{t-1};\Theta)$, for which closed-form formulas are reported in Appendix A, for all probability distributions of this paper. We use the loss functions $\mathrm{SE}_{i,t}=\left[\sigma_t^*-\sigma(y_t|\mathcal{F}_{t-1};\Theta)\right]^2$ and $\mathrm{AE}_{i,t}=|\sigma_t^*-\sigma(y_t|\mathcal{F}_{t-1};\Theta)|$, where i denotes the EGARCH specification for which the conditional volatility is $\sigma(y_t|\mathcal{F}_{t-1};\Theta)$. We note that as alternatives we also use SE and AE loss functions in which $\left(\sigma_t^*\right)^2$ and $\sigma^2(y_t|\mathcal{F}_{t-1};\Theta)$ are included; we obtain similar in-sample forecasting accuracy results to the ones reported in Tables 3–6.

For each probability distribution, we compare the in-sample volatility forecasting performance of the score-driven model with constant shape parameters with that of the score-driven models with time-varying shape parameters. We define $d_t(\mathrm{SE})=\mathrm{SE}_{c,t}-\mathrm{SE}_{d,t}$, where $i=c$ indicates the score-driven model with constant shape parameters and $i=d$ indicates a score-driven model with time-varying shape parameters. We also define $d_t(\mathrm{AE})=\mathrm{AE}_{c,t}-\mathrm{AE}_{d,t}$, where $i=c$ indicates the score-driven model with constant shape parameters and $i=d$ indicates a score-driven model with time-varying shape parameters. We regress $d_t(\mathrm{SE})$ and $d_t(\mathrm{AE})$ on a constant parameter and we estimate its standard error by using the Newey–West heteroskedasticity and autocorrelation consistent (HAC) estimator (Newey and West 1987). A significantly positive estimate of the constant parameter indicates that the in-sample volatility forecasting performance of the score-driven model with dynamic shape parameters is superior to that of the score-driven model with constant shape parameters.

In Tables 3–6, we report the root mean SE (RMSE) and the mean AE (MAE) estimates for each specification, and for those statistics we also report in parentheses the p-values corresponding to the constant parameter in the linear regressions of the aforementioned loss function differences. We find two cases for the score-driven EGARCH models with dynamic shape parameters for which the in-sample volatility forecasting performance is significantly superior to that of the corresponding score-driven EGARCH models with time-invariant shape parameters: (i) score-driven Skew-Gen-t model with dynamic τ_t, dynamic ν_t, and dynamic η_t; (ii) score-driven Skew-Gen-t model with constant τ_t, dynamic ν_t, and dynamic η_t. These specifications are also supported by the LR tests, hence we consider them as the best-performing score-driven EGARCH specifications of the present paper. We note that for the score-driven EGB2 and NIG specifications, the realized volatility-based model performance analysis does not indicate superior performances of the score-driven models with dynamic shape parameters.

4.2 Out-of-sample VaR backtesting

Financial institutions frequently evaluate and update their risk management systems. One of those evaluation methods is the backtesting of VaR models, by which the predictive performance of VaR models is tested by using out-of-sample forecasting and evaluation approaches.

In this section VaR backtesting applications are presented, for which the VaR measurements of the score-driven models with constant and dynamic shape parameters are compared. If the score-driven shape parameters predict tail-shape dynamics, then we will expect that the VaR predictive performance of the score-driven models with dynamic shape parameters is superior to the VaR predictive performance of the score-driven models with constant shape parameters. The results provide the following insight on the S&P 500 for practitioners about the quality of the VaR measurements for the new score-driven specifications. We find that the score-driven models with dynamic shape parameters anticipate better extreme losses than the score-driven models with constant shape parameters.

A. Evolution of $\tanh(\tau_t)$ for the period of February 14, 1990 to October 21, 2021

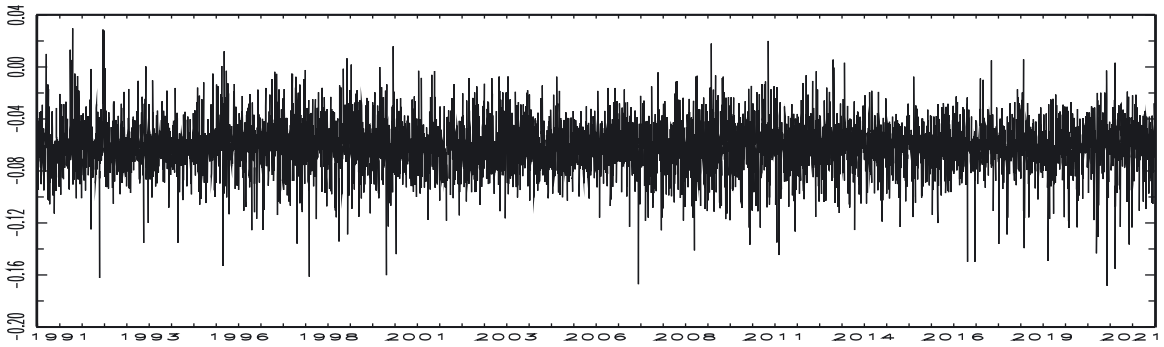

B. Evolution of $\exp(\nu_t) + 4$ for the period of February 14, 1990 to October 21, 2021

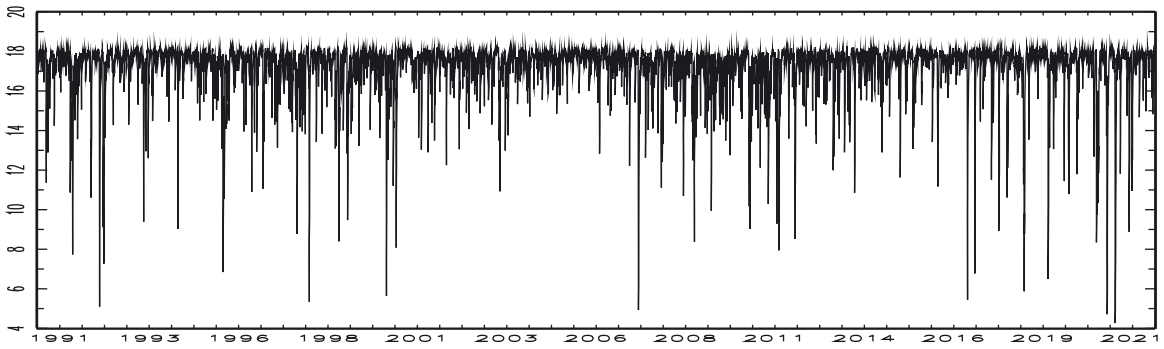

C. Evolution of $\exp(\eta_t)$ for the period of February 14, 1990 to October 21, 2021

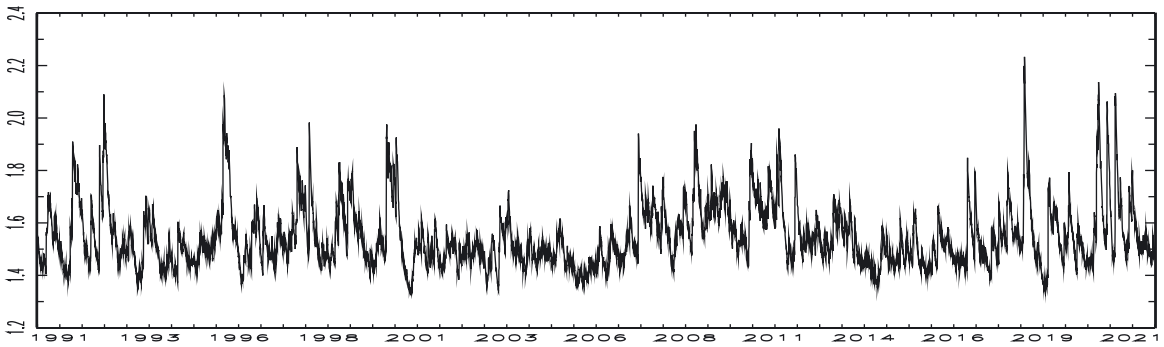

D. Evolution of $\exp(\lambda_t)$ for the period of February 14, 1990 to October 21, 2021

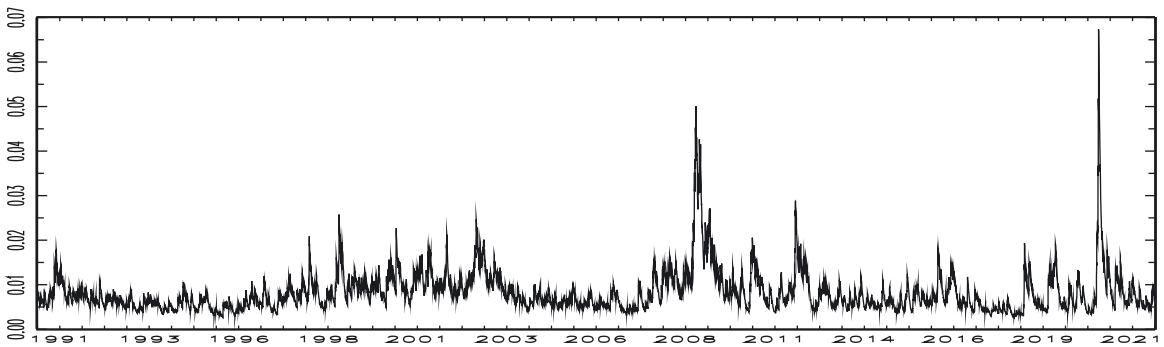

Figure 4: Evolution of the shape and scale parameters for the score-driven Skew-Gen-t model with dynamic shape parameters τ_t, ν_t, and η_t.
The lowest extreme values of ν_t indicate the extreme events (Appendix D).

Extreme observations in the S&P 500 log-returns are concentrated during the period of the dot.com boom, 2008 US Financial Crisis, and COVID-19 pandemic, which are some of the most recent high-volatility periods presented in Appendix D. In Table 2, we present the dates of the periods of the dot.com boom, 2008 US Financial Crisis, and COVID-19 pandemic. Moreover, in Figure 3A and B, we present the concentration of the outliers for those subperiods of the sample. This motivates the consideration of those periods in the VaR backtesting applications. The design of the VaR backtesting procedure of this paper is in accordance with the framework of the Basel Committee (1996), in which a 1 day VaR is estimated out-of-sample at the 99% confidence level. In the present paper, a VaR (1 day, 99%) is estimated for each of the trading days of the backtesting period (Table 2).

An extending-window estimation approach is used for all score-driven models. For all VaR estimates, the first observation of the extending-window is February 14, 1990 and the last observation is for the last trading day before the day of the VaR estimate. VaR is approximated after the parameter estimation by using MC simulations, for which 10,000 possible log-returns are simulated for the trading day after the last observation of each rolling window. VaR (1 day, 99%) is defined by the 1% quantile of the log-return simulations. Motivated by the results presented in Section 4.1, the performance of VaR is compared for the score-driven Skew-Gen-t models with constant and dynamic shape parameters. All shape parameters are time-varying for the dynamic shape filters. See the VaR estimates in Figure 5.

To evaluate the VaR performance of different models, we use the Kupiec test to evaluate whether the proportion of VaR (1 day, 99%) failures is significantly higher than 1% during the backtesting period. The null hypothesis of the Kupiec test is that the observed VaR failure rate is equal to the failure rate suggested by the VaR confidence interval (i.e. 99% in this paper). The Kupiec test statistic is:

$$\text{Kupiec} = -2 \ln \left[\frac{(1-p)^{T_b - X} p^X}{\left(1 - \frac{X}{T_b}\right)^{T_b - X} \left(\frac{X}{T_b}\right)^X} \right] \tag{21}$$

where $p = 1\%$, T_b is the sample size for the backtesting period, and X is the number of VaR failures. Under the null hypothesis, the probability distribution of the Kupiec test statistic is the chi-squared distribution with 1 degrees of freedom.

The number of VaR failures and the Kupiec test results for the dot.com boom, 2008 US Financial Crisis, and COVID-19 pandemic backtesting periods are presented in Table 7. The results indicate a clear difference between the VaR forecasting accuracy of the score-driven EGARCH model with constant shape parameters and the score-driven EGARCH model with dynamic shape parameters: (i) For the score-driven EGARCH model with constant shape parameters, the null hypothesis of the Kupiec test is rejected at the 1% level of significance for the dot.com boom and it is rejected at the 10% level of significance for the 2008 US Financial Crisis and COVID-19 pandemic. (ii) For the score-driven EGARCH model with dynamic shape parameters, the same null hypothesis is never rejected. These results indicate for practitioners that financial institutions or investors can anticipate extreme losses better by using score-driven models with dynamic shape parameters than by using score-driven models with constant shape parameters.

We also performed the Christoffersen test. The null hypothesis of the Christoffersen test is that the arrival times of VaR failures are independent. If that null hypothesis is rejected, for example, due to consecutive VaR failures within the backtesting period, then the econometric model is not updated correctly after extreme observations. For all cases of Table 7 we find that the Christoffersen test does not provide evidence against the model specifications.

The VAR backtesting application indicates that, during periods of high market volatility, the VaR measurements of the score-driven models with dynamic shape parameters are improved, compared to the VaR measurements of the score-driven models with constant shape parameters.

A. VaR for constant shape (thin solid); VaR for dynamic shape (thick solid) for the dot.com boom
(The backtesting period is from January 2, 1997 to October 9, 2002.)

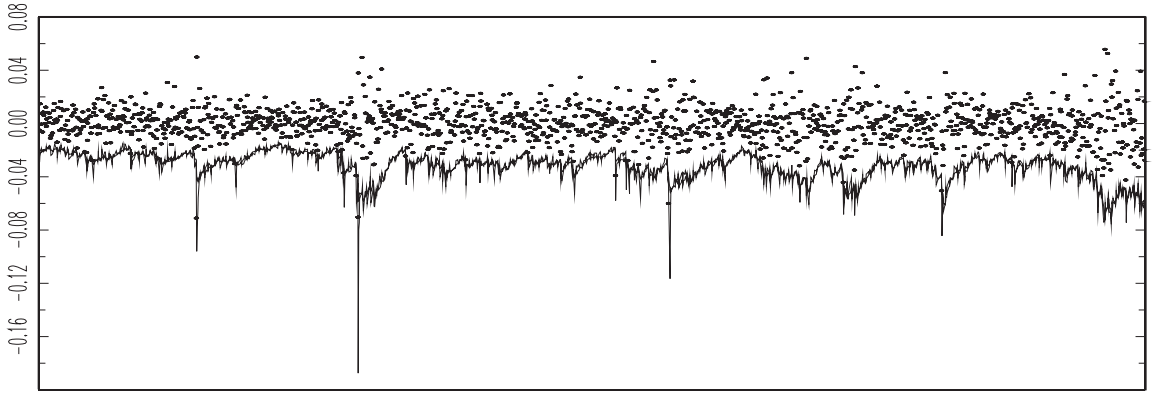

B. VaR for constant shape (thin solid); VaR for dynamic shape (thick solid) for the 2008 US Financial Crisis
(The backtesting period is from October 1, 2007 to March 31, 2009.)

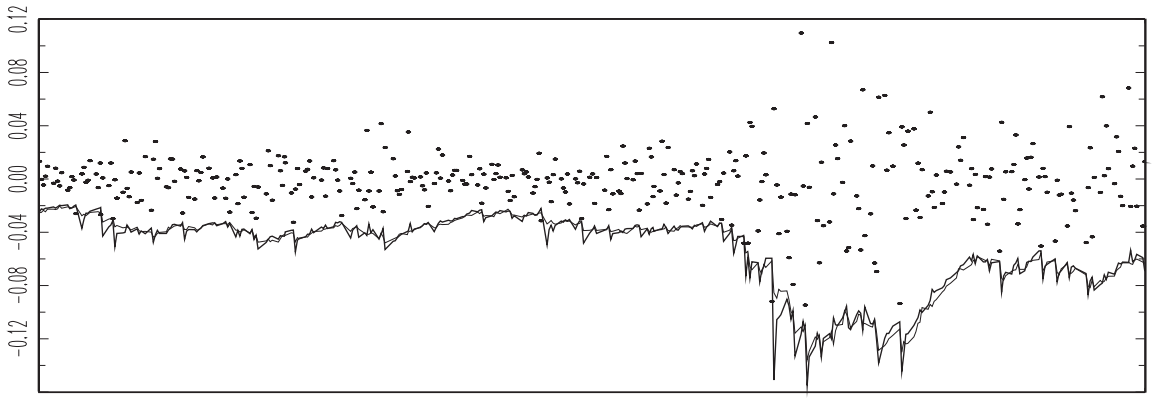

C. VaR for constant shape (thin solid); VaR for dynamic shape (thick solid) for the COVID-19 pandemic
(The backtesting period is from January 9, 2020 to October 21, 2021.)

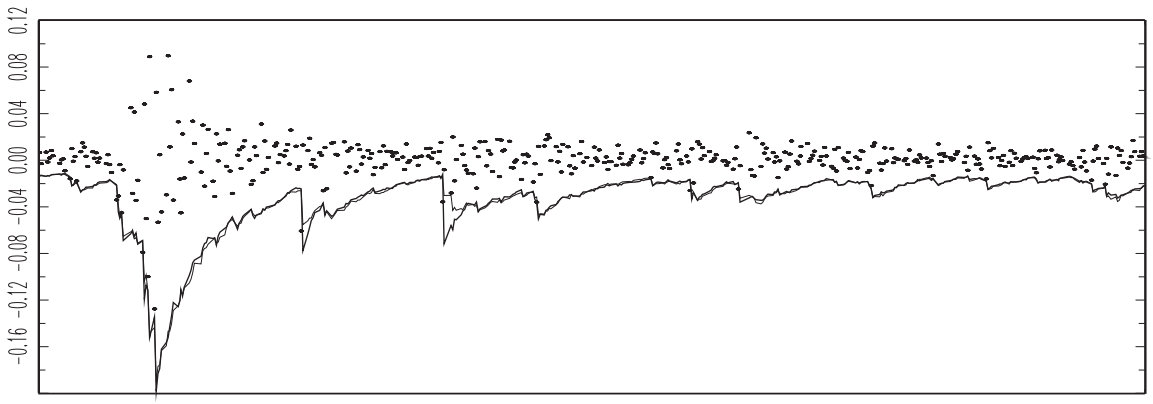

Figure 5: Log-returns on the S&P 500 (solid circles) and out-of-sample VaR (1 day, 99%) estimates for the score-driven Skew-Gen-*t* model are presented. All shape parameters are dynamic for the Skew-Gen-*t* dynamic-shape specification. After an extreme S&P 500 observation, for most of the cases, the VaR for dynamic shape (thick solid) predicts a more severe potential loss than the VaR for constant shape (thin solid). For all out-of-sample VaR estimates we use an expanding window, which starts at February 14, 1990 and ends on the trading day before each VaR estimate.

Table 7: VaR backtesting for the score-driven Skew-Gen-*t* model.

	VaR for constant shape	VaR for dynamic shape
A. dot.com boom		
Pr, probability	1%	1%
X, VaR failures	28	21
T_b sample size for backtesting period	1, 452	1, 452
Kupiec test statistic	9.9407	2.5671
Kupiec test, p-value	0.0016	0.1091
B. 2008 US financial crisis		
Pr, probability	1%	1%
X, VaR failures	8	6
T_b sample size for backtesting period	378	378
Kupiec test statistic	3.6032	1.1176
Kupiec test, p-value	0.0577	0.2904
C. COVID-19 pandemic		
Pr, probability	1%	1%
X, VaR failures	9	7
T_b sample size for backtesting period	451	451
Kupiec test statistic	3.5020	1.1885
Kupiec test, p-value	0.0613	0.2756

Value-at-Risk (VaR); skewed generalized *t*-distribution (Skew-Gen-*t*); United States (US).

5 Conclusions

We have suggested the use of a new econometric method for VaR that anticipates consecutive extreme losses, by using score-driven filters of the shape parameters for the EGB2, NIG, and Skew-Gen-*t* probability distributions. The score-driven shape filters update the tail shape, peakedness, and skewness of the conditional distribution of returns. The score-driven models have been estimated in one step by using the ML method. The consistency of the ML estimator for the shape parameters of the Skew-Gen-*t* model has been supported by performing MC simulation experiments.

As control data, daily log-returns of the S&P 500 index have been used. According to the LR test results, the in-sample statistical performances of the score-driven shape filters have been superior to the in-sample statistical performances of the score-driven models with constant shape parameters. According to the realized volatility-based model performance results, the Skew-Gen-*t* model is superior to the EGB2 and NIG models. VaR backtesting has been performed for the period of the dot.com boom, 2008 US Financial Crisis, and COVID-19 pandemic, by using the backtesting framework of the Basel Committee. The VaR results have indicated that the score-driven models with dynamic shape parameters anticipate extreme losses better than the score-driven models with constant shape parameters.

These results motivate the use of the new econometric method for VaR measurements, in order to properly update the VaR and anticipate potential extreme losses on the portfolios.

Acknowledgement: This paper was presented at the GESG Research Seminar, Universidad Francisco Marroquín (March 7, 2019), Cambridge-INET Conference on Score-Driven and Nonlinear Time Series Models, University of Cambridge (March 27–29, 2019), IX th Workshop in Time Series Econometrics, University of Zaragoza (April 4–5, 2019), and Summer Workshop of the Institute of Economics, Hungarian Academy of Sciences (August 18–19, 2022). The authors are thankful to Matthew Copley, Juan Carlos Escanciano, Andrew Harvey, Jason Jones, Gábor Kőrösi, Róbert Lieli, and conference participants.

Author contributions: All the authors have accepted responsibility for the entire content of this submitted manuscript and approved submission.
Research funding: Ayala and Blazsek acknowledge funding from Universidad Francisco Marroquín. Escribano acknowledges funding from the Spanish Ministry of Economy, Industry and Competitiveness (ECO2015-68715-R, ECO2016-00105-001), Consolidation Grant (#2006/04046/002), and Maria de Maeztu Grant (MDM 2014-0431).
Conflict of interest statement: The authors declare no conflicts of interest regarding this article.

Appendix A

In this appendix, for each error specification, the conditional distribution of ϵ_t, the first four conditional moments of ϵ_t, the conditional distribution of y_t, the conditional mean of y_t, the conditional volatility of y_t, the log of the conditional density of y_t, the scaled score function for location $u_{\mu,t}$, and the score functions for scale $u_{\lambda,t}$ and shape $u_{\rho,k,t}$ are presented.

(i) For the score-driven EGB2 model, $\epsilon_t|\mathcal{F}_{t-1} \sim \text{EGB2}[0, 1, \exp(\xi_t), \exp(\zeta_t)]$, where the distribution is conditional on $\mathcal{F}_{t-1} = [\mu_1, \lambda_1, (\rho_{1,1}, \dots, \rho_{K,1}), (y_1, \dots, y_{t-1})]$. The conditional mean, conditional variance, conditional skewness, and conditional kurtosis of ϵ_t are given by:

$$E(\epsilon_t|\mathcal{F}_{t-1};\Theta) = \Psi^{(0)}[\exp(\xi_t)] - \Psi^{(0)}[\exp(\zeta_t)] \tag{A.1}$$

$$\text{Var}(\epsilon_t|\mathcal{F}_{t-1};\Theta) = \Psi^{(1)}[\exp(\xi_t)] + \Psi^{(1)}[\exp(\zeta_t)] \tag{A.2}$$

$$\text{Skew}(\epsilon_t|\mathcal{F}_{t-1};\Theta) = \Psi^{(2)}[\exp(\xi_t)] - \Psi^{(2)}[\exp(\zeta_t)] \tag{A.3}$$

$$\text{Kurt}(\epsilon_t|\mathcal{F}_{t-1};\Theta) = \Psi^{(3)}[\exp(\xi_t)] + \Psi^{(3)}[\exp(\zeta_t)] \tag{A.4}$$

respectively, where Θ is the vector of parameters and $\Psi^{(i)}(x)$ is the polygamma function of order i. For the score-driven EGB2 model, $y_t|\mathcal{F}_{t-1} \sim \text{EGB2}[\mu_t, \exp(-\lambda_t), \exp(\xi_t), \exp(\zeta_t)]$. The conditional mean and the conditional volatility of y_t are

$$E(y_t|\mathcal{F}_{t-1};\Theta) = \mu_t + \exp(\lambda_t)\left\{\Psi^{(0)}[\exp(\xi_t)] - \Psi^{(0)}[\exp(\zeta_t)]\right\} \tag{A.5}$$

$$\sigma(y_t|\mathcal{F}_{t-1};\Theta) = \exp(\lambda_t)\left\{\Psi^{(1)}[\exp(\xi_t)] + \Psi^{(1)}[\exp(\zeta_t)]\right\}^{1/2} \tag{A.6}$$

respectively. The log of the conditional density of y_t is

$$\begin{aligned}\ln\ f(y_t|\mathcal{F}_{t-1};\Theta) = {} & \exp(\xi_t)\epsilon_t - \lambda_t - \ln\Gamma[\exp(\xi_t)] - \ln\Gamma[\exp(\zeta_t)] \\ & + \ln\Gamma[\exp(\xi_t) + \exp(\zeta_t)] - [\exp(\xi_t) + \exp(\zeta_t)]\ln[1 + \exp(\epsilon_t)]\end{aligned} \tag{A.7}$$

The score functions with respect to μ_t, λ_t, ξ_t, and ζ_t are as follows. First, the score function with respect to μ_t is

$$\frac{\partial\ \ln\ f(y_t|\mathcal{F}_{t-1};\Theta)}{\partial\mu_t} = u_{\mu,t} \times \left\{\Psi^{(1)}[\exp(\xi_t)] + \Psi^{(1)}[\exp(\zeta_t)]\right\}\exp(2\lambda_t) = u_{\mu,t} \times k_t \tag{A.8}$$

where

$$u_{\mu,t} = \left\{\Psi^{(1)}[\exp(\xi_t)] + \Psi^{(1)}[\exp(\zeta_t)]\right\}\exp(\lambda_t)\left\{[\exp(\xi_t) + \exp(\zeta_t)]\frac{\exp(\epsilon_t)}{\exp(\epsilon_t)+1} - \exp(\xi_t)\right\} \tag{A.9}$$

is the scaled score function. Second, the score function with respect to λ_t is

$$u_{\lambda,t} = \frac{\partial\ \ln\ f(y_t|\mathcal{F}_{t-1};\Theta)}{\partial\lambda_t} = [\exp(\xi_t) + \exp(\zeta_t)]\frac{\epsilon_t\ \exp(\epsilon_t)}{\exp(\epsilon_t)+1} - \exp(\xi_t)\epsilon_t - 1 \tag{A.10}$$

Third, the score function with respect to ξ_t is

$$u_{\xi,t} = \frac{\partial \ln f(y_t|\mathcal{F}_{t-1};\Theta)}{\partial \xi_t} = \exp(\xi_t)\epsilon_t - \exp(\xi_t)\Psi^{(0)}[\exp(\xi_t)] + \exp(\xi_t)\Psi^{(0)}[\exp(\xi_t)+\exp(\zeta_t)] - \exp(\xi_t)\ln[1+\exp(\epsilon_t)] \tag{A.11}$$

Fourth, the score function with respect to ζ_t is

$$u_{\zeta,t} = \frac{\partial \ln f(y_t|\mathcal{F}_{t-1};\Theta)}{\partial \zeta_t} = -\exp(\zeta_t)\Psi^{(0)}[\exp(\zeta_t)] + \exp(\zeta_t)\Psi^{(0)}[\exp(\xi_t)+\exp(\zeta_t)] - \exp(\zeta_t)\ln[1+\exp(\epsilon_t)] \tag{A.12}$$

(ii) For the score-driven NIG model, $\epsilon_t|\mathcal{F}_{t-1} \sim \text{NIG}[0,1,\exp(\nu_t),\exp(\nu_t)\tanh(\eta_t)]$, where $\tanh(x)$ is the hyperbolic tangent function. The conditional mean, conditional variance, conditional skewness, and conditional kurtosis of ϵ_t are given by:

$$E(\epsilon_t|\mathcal{F}_{t-1};\Theta) = \frac{\tanh(\eta_t)}{\left[1-\tanh^2(\eta_t)\right]^{1/2}} \tag{A.13}$$

$$\text{Var}(\epsilon_t|\mathcal{F}_{t-1};\Theta) = \frac{\exp(-\nu_t)}{\left[1-\tanh^2(\eta_t)\right]^{3/2}} \tag{A.14}$$

$$\text{Skew}(\epsilon_t|\mathcal{F}_{t-1};\Theta) = \frac{3\ \tanh(\eta_t)}{\exp(\nu_t/2)\left[1-\tanh^2(\eta_t)\right]^{1/4}} \tag{A.15}$$

$$\text{Kurt}(\epsilon_t|\mathcal{F}_{t-1};\Theta) = 3 + \frac{3\left[1+4\ \tanh^2(\eta_t)\right]}{\exp(\nu_t)\left[1-\tanh^2(\eta_t)\right]^{1/2}} \tag{A.16}$$

respectively. For the score-driven NIG model, the conditional distribution of y_t is

$$y_t|\mathcal{F}_{t-1} \sim \text{NIG}[\mu_t,\exp(\lambda_t),\exp(\nu_t-\lambda_t),\exp(\nu_t-\lambda_t)\tanh(\eta_t)] \tag{A.17}$$

The conditional mean and the conditional volatility of y_t are

$$E(y_t|\mathcal{F}_{t-1};\Theta) = \mu_t + \frac{\exp(\lambda_t)\tanh(\eta_t)}{\left[1-\tanh^2(\eta_t)\right]^{1/2}} \tag{A.18}$$

$$\sigma(y_t|\mathcal{F}_{t-1};\Theta) = \left\{\frac{\exp(2\lambda_t-\nu_t)}{\left[1-\tanh^2(\eta_t)\right]^{3/2}}\right\}^{1/2} \tag{A.19}$$

respectively. The log of the conditional density of y_t is

$$\ln f(y_t|\mathcal{F}_{t-1};\Theta) = \nu_t - \lambda_t - \ln(\pi) + \exp(\nu_t)\left[1-\tanh^2(\eta_t)\right]^{1/2} + \exp(\nu_t)\tanh(\eta_t)\epsilon_t + \ln K^{(1)}\left[\exp(\nu_t)\sqrt{1+\epsilon_t^2}\right] - \frac{1}{2}\ln\left(1+\epsilon_t^2\right) \tag{A.20}$$

where $K^{(1)}(x)$ is the modified Bessel function of the second kind of order 1. The score functions with respect to μ_t, λ_t, ν_t, and η_t are as follows. First, the score function with respect to μ_t is

$$\frac{\partial \ln f(y_t|\mathcal{F}_{t-1};\Theta)}{\partial \mu_t} = -\exp(\nu_t - \lambda_t)\tanh(\eta_t) + \frac{\epsilon_t}{\exp(\lambda_t)(1+\epsilon_t^2)} + \frac{\exp(\nu_t - \lambda_t)\epsilon_t}{\sqrt{1+\epsilon_t^2}} \times \frac{K^{(0)}\left[\exp(\nu_t)\sqrt{1+\epsilon_t^2}\right] + K^{(2)}\left[\exp(\nu_t)\sqrt{1+\epsilon_t^2}\right]}{2K^{(1)}\left[\exp(\nu_t)\sqrt{1+\epsilon_t^2}\right]} \tag{A.21}$$

where $K^{(0)}(x)$ and $K^{(2)}(x)$ are the modified Bessel functions of the second kind of orders 0 and 2, respectively. Define the scaled score function with respect to μ_t as

$$u_{\mu,t} = \frac{\partial \ln f(y_t|\mathcal{F}_{t-1};\Theta)}{\partial \mu_t} \times \exp(2\lambda_t) = \frac{\partial \ln f(y_t|\mathcal{F}_{t-1};\Theta)}{\partial \mu_t} \times k_t^{-1} \tag{A.22}$$

Second, the score function with respect to λ_t is

$$u_{\lambda,t} = \frac{\partial \ln f(y_t|\mathcal{F}_{t-1};\Theta)}{\partial \lambda_t} = -1 - \exp(\nu_t)\tanh(\eta_t)\epsilon_t + \frac{\epsilon_t^2}{1+\epsilon_t^2} + \frac{\exp(\nu_t)\epsilon_t^2}{\sqrt{1+\epsilon_t^2}} \times \frac{K^{(0)}\left[\exp(\nu_t)\sqrt{1+\epsilon_t^2}\right] + K^{(2)}\left[\exp(\nu_t)\sqrt{1+\epsilon_t^2}\right]}{2K^{(1)}\left[\exp(\nu_t)\sqrt{1+\epsilon_t^2}\right]} \tag{A.23}$$

Third, the score function with respect to ν_t is

$$u_{\nu,t} = \frac{\partial \ln f(y_t|\mathcal{F}_{t-1};\Theta)}{\partial \nu_t} = 1 + \exp(\nu_t)\left[1-\tanh^2(\eta_t)\right]^{1/2} + \exp(\nu_t)\tanh(\eta_t)\epsilon_t - \exp(\nu_t)\sqrt{1+\epsilon_t^2} \times \frac{K^{(0)}\left[\exp(\nu_t)\sqrt{1+\epsilon_t^2}\right] + K^{(2)}\left[\exp(\nu_t)\sqrt{1+\epsilon_t^2}\right]}{2K^{(1)}\left[\exp(\nu_t)\sqrt{1+\epsilon_t^2}\right]} \tag{A.24}$$

Fourth, the score function with respect to η_t is

$$u_{\eta,t} = \frac{\partial \ln f(y_t|\mathcal{F}_{t-1};\Theta)}{\partial \eta_t} = \exp(\nu_t)\text{sech}^2(\eta_t)\epsilon_t - \exp(\nu_t)\tanh(\eta_t)\text{sech}(\eta_t) \tag{A.25}$$

where $\text{sech}(x)$ is the hyperbolic secant function.

(iii) For the score-driven Skew-Gen-t model, $\epsilon_t|\mathcal{F}_{t-1} \sim \text{Skew}-\text{Gen}-t[0, 1, \tanh(\tau_t), \exp(\nu_t)+4, \exp(\eta_t)]$. The conditional mean, conditional variance, conditional skewness, and conditional kurtosis of ϵ_t, respectively, are:

$$E(\epsilon_t|\mathcal{F}_{t-1};\Theta) = \frac{2\tanh(\tau_t)[\exp(\nu_t)+4]^{\exp(-\eta_t)}\, B\left\{\frac{2}{\exp(\eta_t)}, \frac{\exp(\nu_t)+3}{\exp(\eta_t)}\right\}}{B\left\{\frac{1}{\exp(\eta_t)}, \frac{\exp(\nu_t)+4}{\exp(\eta_t)}\right\}} \tag{A.26}$$

$$\text{Var}(\epsilon_t|\mathcal{F}_{t-1};\Theta) = [\exp(\nu_t)+4]^{2\ \exp(-\eta_t)} \times \left\{ \frac{\left[3\ \tanh^2(\tau_t)+1\right]B\left[\frac{3}{\exp(\eta_t)}, \frac{\exp(\nu_t)+2}{\exp(\eta_t)}\right]}{B\left[\frac{1}{\exp(\eta_t)}, \frac{\exp(\nu_t)+4}{\exp(\eta_t)}\right]} - \frac{4\ \tanh^2(\tau_t)B^2\left[\frac{2}{\exp(\eta_t)}, \frac{\exp(\nu_t)+3}{\exp(\eta_t)}\right]}{B^2\left[\frac{1}{\exp(\eta_t)}, \frac{\exp(\nu_t)+4}{\exp(\eta_t)}\right]} \right\} \tag{A.27}$$

$$\text{Skew}(\epsilon_t|\mathcal{F}_{t-1};\Theta) = \frac{2\ \tanh(\tau_t)[\exp(\nu_t)+4]^{3\ \exp(-\eta_t)}}{B^3\left[\frac{1}{\exp(\eta_t)},\frac{\exp(\nu_t)+4}{\exp(\eta_t)}\right]} \tag{A.28}$$
$$\times\left\{8\ \tanh^2(\tau_t)B^3\left[\frac{2}{\exp(\eta_t)},\frac{\exp(\nu_t)+3}{\exp(\eta_t)}\right]-3\left[1+3\ \tanh^2(\tau_t)\right]B\right.$$
$$\times\left[\frac{1}{\exp(\eta_t)},\frac{\exp(\nu_t)+4}{\exp(\eta_t)}\right]B\left[\frac{2}{\exp(\eta_t)},\frac{\exp(\nu_t)+3}{\exp(\eta_t)}\right]B\left[\frac{3}{\exp(\eta_t)},\frac{\exp(\nu_t)+2}{\exp(\eta_t)}\right]$$
$$\left.+2\left[1+\tanh^2(\tau_t)\right]B^2\left[\frac{1}{\exp(\eta_t)},\frac{\exp(\nu_t)+4}{\exp(\eta_t)}\right]B\left[\frac{4}{\exp(\eta_t)},\frac{\exp(\nu_t)+1}{\exp(\eta_t)}\right]\right\}$$

$$\text{Kurt}(\epsilon_t|\mathcal{F}_{t-1};\Theta) = \frac{[\exp(\nu_t)+4]^{4\ \exp(-\eta_t)}}{B^4\left[\frac{1}{\exp(\eta_t)},\frac{\exp(\nu_t)+4}{\exp(\eta_t)}\right]}\left\{-48\ \tanh^4(\tau_t)B^4\left[\frac{2}{\exp(\eta_t)},\frac{\exp(\nu_t)+3}{\exp(\eta_t)}\right]\right. \tag{A.29}$$
$$+24\ \tanh^2(\tau_t)\left[1+3\ \tanh^2(\tau_t)\right]B\left[\frac{1}{\exp(\eta_t)},\frac{\exp(\nu_t)+4}{\exp(\eta_t)}\right]B^2\left[\frac{2}{\exp(\eta_t)},\frac{\exp(\nu_t)+3}{\exp(\eta_t)}\right]$$
$$\times B\left[\frac{3}{\exp(\eta_t)},\frac{\exp(\nu_t)+2}{\exp(\eta_t)}\right]-32\ \tanh^2(\tau_t)\left[1+\tanh^2(\tau_t)\right]B^2\left[\frac{1}{\exp(\eta_t)},\frac{\exp(\nu_t)+4}{\exp(\eta_t)}\right]$$
$$\times B\left[\frac{2}{\exp(\eta_t)},\frac{\exp(\nu_t)+3}{\exp(\eta_t)}\right]B\left[\frac{4}{\exp(\eta_t)},\frac{\exp(\nu_t)+1}{\exp(\eta_t)}\right]$$
$$\left.+\left[1+10\ \tanh^2(\tau_t)+5\ \tanh^4(\tau_t)\right]B^3\left[\frac{1}{\exp(\eta_t)},\frac{\exp(\nu_t)+4}{\exp(\eta_t)}\right]B\left[\frac{5}{\exp(\eta_t)},\frac{\exp(\nu_t)}{\exp(\eta_t)}\right]\right\}$$

respectively; $B(x,y)=\Gamma(x)\Gamma(y)/\Gamma(x+y)$ is the beta function. For the score-driven Skew-Gen-t model, the conditional distribution of y_t is

$$y_t|\mathcal{F}_{t-1} \sim \text{Skew}-\text{Gen}-t[\mu_t,\exp(\lambda_t),\tanh(\tau_t),\exp(\nu_t)+4,\exp(\eta_t)] \tag{A.30}$$

The conditional mean of y_t is

$$E(y_t|\mathcal{F}_{t-1};\Theta) = \mu_t + 2\exp(\lambda_t)\tanh(\tau_t)[\exp(\nu_t)+4]^{\exp(-\eta_t)} \times \frac{B\left\{\frac{2}{\exp(\eta_t)},\frac{\exp(\nu_t)+3}{\exp(\eta_t)}\right\}}{B\left\{\frac{1}{\exp(\eta_t)},\frac{\exp(\nu_t)+4}{\exp(\eta_t)}\right\}} \tag{A.31}$$

The conditional volatility of y_t is

$$\sigma(y_t|\mathcal{F}_{t-1};\Theta) = \exp(\lambda_t)[\exp(\nu_t)+4]^{\exp(-\eta_t)} \tag{A.32}$$
$$\times\left\{\frac{\left[3\ \tanh^2(\tau_t)+1\right]B\left[\frac{3}{\exp(\eta_t)},\frac{\exp(\nu_t)+2}{\exp(\eta_t)}\right]}{B\left[\frac{1}{\exp(\eta_t)},\frac{\exp(\nu_t)+4}{\exp(\eta_t)}\right]}-\frac{4\ \tanh^2(\tau_t)B^2\left[\frac{2}{\exp(\eta_t)},\frac{\exp(\nu_t)+3}{\exp(\eta_t)}\right]}{B^2\left[\frac{1}{\exp(\eta_t)},\frac{\exp(\nu_t)+4}{\exp(\eta_t)}\right]}\right\}^{1/2}$$

The log of the conditional density of y_t is

$$\ln\ f(y_t|\mathcal{F}_{t-1};\Theta) = \eta_t-\lambda_t-\ln(2)-\frac{\ln[\exp(\nu_t)+4]}{\exp(\eta_t)}-\ln\Gamma\left[\frac{\exp(\nu_t)+4}{\exp(\eta_t)}\right]-\ln\Gamma[\exp(-\eta_t)] \tag{A.33}$$
$$+\ln\Gamma\left[\frac{\exp(\nu_t)+5}{\exp(\eta_t)}\right]-\frac{\exp(\nu_t)+5}{\exp(\eta_t)}\ln\left\{1+\frac{|\epsilon_t|^{\exp(\eta_t)}}{[1+\tanh(\tau_t)\,\text{sgn}(\epsilon_t)]^{\exp(\eta_t)}\times[\exp(\nu_t)+4]}\right\}$$

First, the score function with respect to μ_t is

$$\frac{\partial \ln f(y_t|\mathcal{F}_{t-1};\Theta)}{\partial \mu_t} = \frac{[\exp(\nu_t)+4]\exp(\lambda_t)\epsilon_t|\epsilon_t|^{\exp(\eta_t)-2}}{|\epsilon_t|^{\exp(\eta_t)}+[1+\tanh(\tau_t)\,\mathrm{sgn}(\epsilon_t)]^{\exp(\eta_t)}[\exp(\nu_t)+4]} \times \frac{\exp(\nu_t)+5}{[\exp(\nu_t)+4]\exp(2\lambda_t)} \tag{A.34}$$

$$= u_{\mu,t} \times \frac{\exp(\nu_t)+5}{[\exp(\nu_t)+4]\exp(2\lambda_t)} = u_{\mu,t} \times k_t$$

where $u_{\mu,t}$ is the scaled score function. Second, the score function with respect to λ_t is

$$u_{\lambda,t} = \frac{\partial \ln f(y_t|\mathcal{F}_{t-1};\Theta)}{\partial \lambda_t} = \frac{|\epsilon_t|^{\exp(\eta_t)}[\exp(\nu_t)+5]}{|\epsilon_t|^{\exp(\eta_t)}+[1+\tanh(\tau_t)\,\mathrm{sgn}(\epsilon_t)]^{\exp(\eta_t)}[\exp(\nu_t)+4]} - 1 \tag{A.35}$$

Third, the score function with respect to τ_t is

$$u_{\tau,t} = \frac{\partial \ln f(y_t|\mathcal{F}_{t-1};\Theta)}{\partial \tau_t} = \frac{[\exp(\nu_t)+5]|\epsilon_t|^{\exp(\eta_t)}\,\mathrm{sgn}(\epsilon_t)\mathrm{sech}(\tau_t)}{[\mathrm{sgn}(\epsilon_t)\sinh(\tau_t)+\cosh(\tau_t)]} \tag{A.36}$$
$$\times \left\{ |\epsilon_t|^{\exp(\eta_t)}+[1+\tanh(\tau_t)\,\mathrm{sgn}(\epsilon_t)]^{\exp(\eta_t)}[\exp(\nu_t)+4] \right\}^{-1}$$

Fourth, the score function with respect to ν_t is

$$u_{\nu,t} = \frac{\partial \ln f(y_t|\mathcal{F}_{t-1};\Theta)}{\partial \nu_t} = -\frac{\exp(\nu_t-\eta_t)}{\exp(\nu_t)+4} - \exp(\nu_t-\eta_t)\Psi^{(0)}\left[\frac{\exp(\nu_t)+4}{\exp(\eta_t)}\right] \tag{A.37}$$
$$+ \exp(\nu_t-\eta_t)\Psi^{(0)}\left[\frac{\exp(\nu_t)+5}{\exp(\eta_t)}\right]$$
$$+ \frac{\exp(\nu_t-\eta_t)[\exp(\nu_t)+5]|\epsilon_t|^{\exp(\eta_t)}}{[\exp(\nu_t)+4]\left\{|\epsilon_t|^{\exp(\eta_t)}+[1+\tanh(\tau_t)\,\mathrm{sgn}(\epsilon_t)]^{\exp(\eta_t)}[\exp(\nu_t)+4]\right\}}$$
$$- \exp(\nu_t-\eta_t)\ln\left\{1+\frac{|\epsilon_t|^{\exp(\eta_t)}}{[1+\tanh(\tau_t)\,\mathrm{sgn}(\epsilon_t)]^{\exp(\eta_t)}[\exp(\nu_t)+4]}\right\}$$

Fifth, the score function with respect to η_t is

$$u_{\eta,t} = \frac{\partial \ln f(y_t|\mathcal{F}_{t-1};\Theta)}{\partial \eta_t} = 1 + \frac{\ln[\exp(\nu_t)+4]}{\exp(\eta_t)} + \frac{\exp(\nu_t)+4}{\exp(\eta_t)}\Psi^{(0)}\left[\frac{\exp(\nu_t)+4}{\exp(\eta_t)}\right] \tag{A.38}$$
$$+ \frac{1}{\exp(\eta_t)}\Psi^{(0)}\left[\frac{1}{\exp(\eta_t)}\right] - \frac{\exp(\nu_t)+5}{\exp(\eta_t)}\Psi^{(0)}\left[\frac{\exp(\nu_t)+5}{\exp(\eta_t)}\right]$$
$$+ \frac{\exp(\nu_t)+5}{\exp(\eta_t)}\ln\left\{1+\frac{|\epsilon_t|^{\exp(\eta_t)}[1+\tanh(\tau_t)\,\mathrm{sgn}(\epsilon_t)]^{-\exp(\eta_t)}}{\exp(\nu_t)+4}\right\}$$
$$+ \frac{[\exp(\nu_t)+5]|\epsilon_t|^{\exp(\eta_t)}\ln[1+\tanh(\tau_t)\,\mathrm{sgn}(\epsilon_t)]}{|\epsilon_t|^{\exp(\eta_t)}+[\exp(\nu_t)+4][1+\tanh(\tau_t)\,\mathrm{sgn}(\epsilon_t)]^{\exp(\eta_t)}}$$
$$- \frac{[\exp(\nu_t)+5]|\epsilon_t|^{\exp(\eta_t)}\ln(|\epsilon_t|)}{|\epsilon_t|^{\exp(\eta_t)}+[\exp(\nu_t)+4][1+\tanh(\tau_t)\,\mathrm{sgn}(\epsilon_t)]^{\exp(\eta_t)}}$$

Appendix B

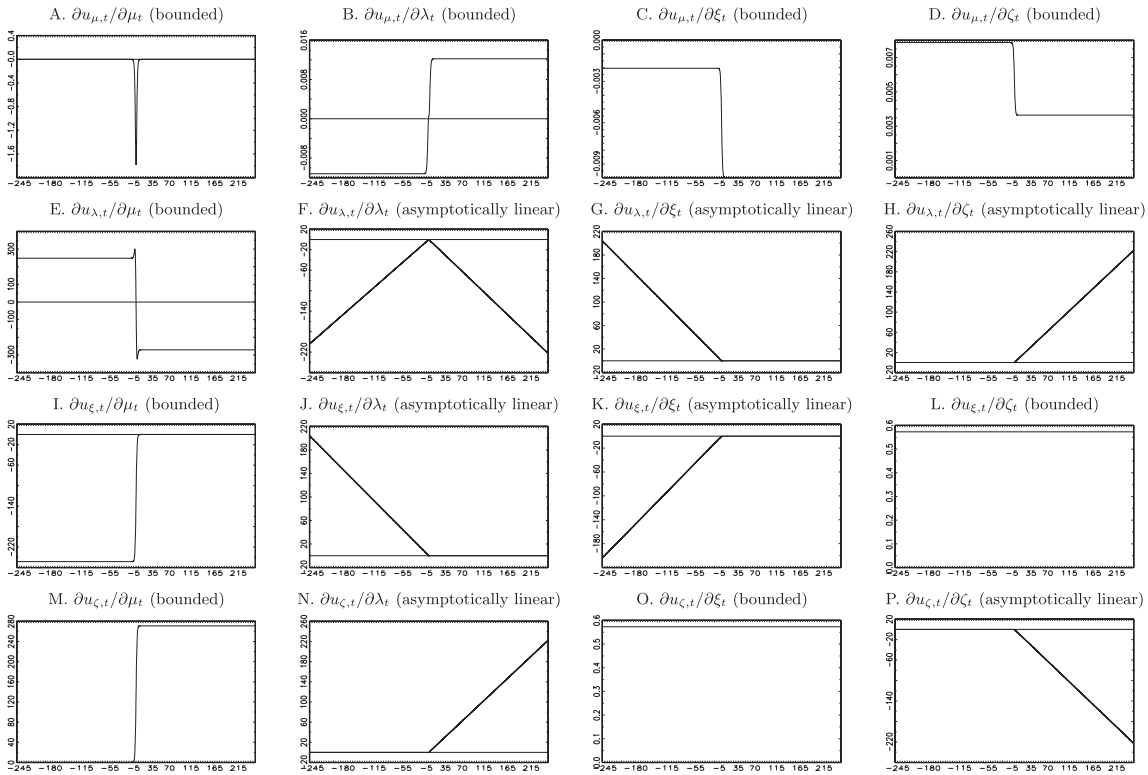

Figure B1: Derivatives of score functions for the EGB2 model with score-driven location, scale, and shape parameters, as a function of $\epsilon_t \in [-250, 250]$.

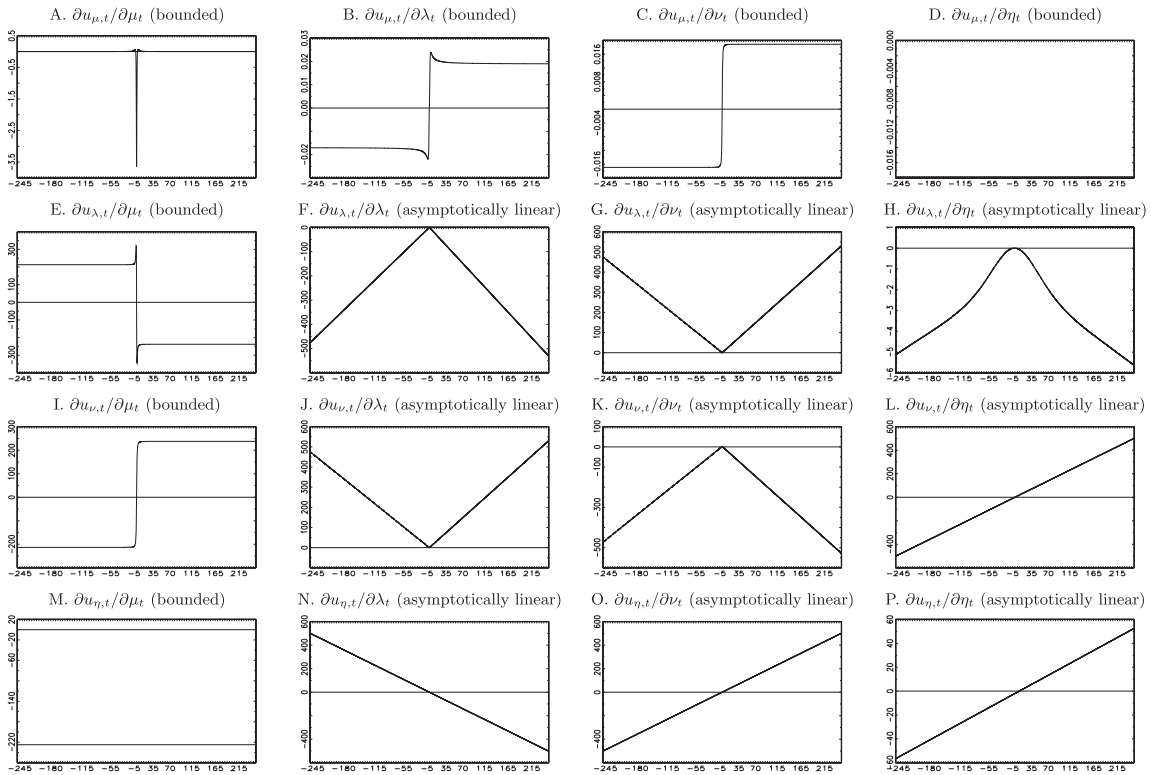

Figure B2: Derivatives of score functions for the NIG model with score-driven location, scale, and shape parameters, as a function of $\epsilon_t \in [-250, 250]$.

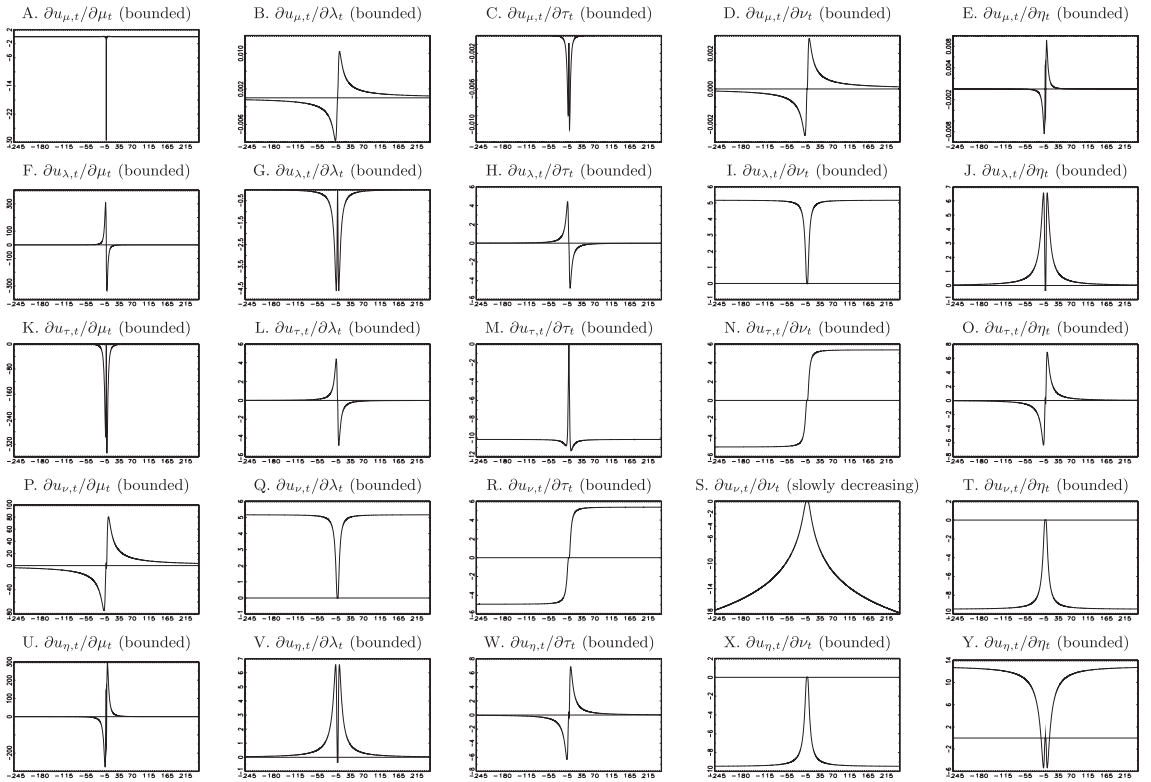

Figure B3: Derivatives of score functions for the Skew-Gen-*t* model with score-driven location, scale, and shape parameters, as a function of $\epsilon_t \in [-250, 250]$.

Appendix C

Table C1: ML estimates for the score-driven EGB2 models for the period of February 14, 1990 to October 21, 2021.

Constant ξ_t and ζ_t		Dynamic ξ_t and ζ_t		Dynamic ξ_t and constant ζ_t		Constant ξ_t and dynamic ζ_t	
C	0.0004*** (0.0002)	c	0.0021*** (0.0003)	c	0.0004*** (0.0001)	C	0.0012 (0.0086)
Φ	0.6539*** (0.1326)	ϕ	−0.8831*** (0.1457)	ϕ	0.6315*** (0.1113)	Φ	−0.0518 (7.5663)
Θ	−0.0292*** (0.0088)	θ	−0.0061 (0.0063)	θ	−0.0443*** (0.0110)	Θ	−0.0009 (0.0126)
Ω	−0.0853*** (0.0132)	ω	−0.0742*** (0.0123)	ω	−0.0759*** (0.0126)	Ω	−0.0793*** (0.0127)
α	0.0453*** (0.0035)	α	0.0460*** (0.0035)	α	0.0443*** (0.0035)	α	0.0463*** (0.0035)
α^*	0.0387*** (0.0026)	α^*	0.0346*** (0.0028)	α^*	0.0367*** (0.0027)	α^*	0.0359*** (0.0026)
β	0.9854*** (0.0024)	β	0.9873*** (0.0022)	β	0.9870*** (0.0022)	β	0.9864*** (0.0023)
λ_0	−5.6400*** (0.4698)	λ_0	−5.6505*** (0.4546)	λ_0	−5.6405*** (0.4703)	λ_0	−5.6292*** (0.5142)
δ_1	−0.4387*** (0.0934)	δ_1	−0.2372 + (0.1521)	δ_1	−0.2291** (0.1153)	δ_1	−0.4276*** (0.0934)
		γ_1	0.4234 (0.3429)	γ_1	0.4500*(0.2454)		
		κ_1	0.0240** (0.0116)	κ_1	0.0357*** (0.0131)		
δ_2	−0.3123*** (0.1013)	δ_2	−0.0966** (0.0432)	δ_2	−0.2987*** (0.1014)	δ_2	−0.1035** (0.0486)
		γ_2	0.6640*** (0.0924)			γ_2	0.6535*** (0.1124)
		κ_2	−0.0628*** (0.0136)			κ_2	−0.0576*** (0.0172)
MDS (mean)	0.8029 (0.3702)	MDS (mean)	0.7736 (0.3791)	MDS (mean)	0.0369 (0.8478)	MDS (mean)	2.8793 (0.0897)
MDS (variance)	0.0013 (0.9715)	MDS (variance)	0.0058 (0.9394)	MDS (variance)	0.1999 (0.6548)	MDS (variance)	0.0077 (0.9301)
MDS (skewness)	0.2592 (0.6106)	MDS (skewness)	2.2834 (0.1308)	MDS (skewness)	17.2194 (0.0000)	MDS (skewness)	1.8826 (0.1700)
MDS (kurtosis)	0.9107 (0.3399)	MDS (kurtosis)	1.2500 (0.2636)	MDS (kurtosis)	7.2019 (0.0073)	MDS (kurtosis)	1.9174 (0.1661)
LL	3.3275	LL	3.3287	LL	3.3280	LL	3.3283
LR	19.2846 (0.0007)	LR	NA	LR	12.3704 (0.0021)	LR	6.0215 (0.0493)

Exponential generalized beta distribution of the second kind (EGB2); martingale difference sequence (MDS); log-likelihood (LL); likelihood-ratio (LR); not available (NA); realized volatility (RV); root mean squared error (RMSE); mean absolute error (MAE). ** and *** indicate significance at the 5 and 1% levels, respectively. For the parameter estimates standard errors are reported in parentheses. For all other statistics of the table, p-values are reported in parentheses. The null hypothesis of the MDS test is the correctness of the EGB2 specification, which is checked up to the first four conditional moments. For the LR test, the most general model is the score-driven model for which all shape parameters are time-varying; the rest of the specifications are special cases, so the classical LR test can be used. Model specification: $y_t = \mu_t + \exp(\lambda_t)\,\epsilon_t$, $\epsilon_t \sim \text{EGB2}[0, 1, \exp(\xi_t), \exp(\zeta_t)]$, $\mu_t = c + \phi\mu_{t-1} + \theta u_{\mu,t-1}$, and $\lambda_t = \omega + \beta\lambda_{t-1} + \alpha u_{\lambda,t-1} + \alpha^* \operatorname{sgn}(-\epsilon_{t-1})\,(u_{\lambda,t-1} + 1)$. For constant ξ_t or ζ_t: $\xi_t = \delta_1$ and $\zeta_t = \delta_2$. For dynamic ξ_t or ζ_t: $\xi_t = \delta_1 + \gamma_1\xi_{t-1} + \kappa_1 u_{\xi,t-1}$ and $\zeta_t = \delta_2 + \gamma_2\zeta_{t-1} + \kappa_2 u_{\zeta,t-1}$.

Table C2: Parameter estimates for the score-driven NIG models for the period of February 14, 1990 to October 21, 2021.

Constant ν_t and η_t		Dynamic ν_t and η_t		Dynamic ν_t and constant η_t		Constant ν_t and dynamic η_t	
c	0.0004^{**} (0.0002)	c	0.0005^{*} (0.0003)	c	0.0004^{***} (0.0002)	c	0.0005^{***} (0.0002)
ϕ	0.6527^{***} (0.1369)	ϕ	0.6052^{***} (0.2060)	ϕ	0.6466^{***} (0.1355)	ϕ	0.6023^{***} (0.1395)
θ	-0.0164^{***} (0.0052)	θ	-0.0146^{**} (0.0060)	θ	-0.0168^{***} (0.0052)	θ	-0.0235^{***} (0.0082)
ω	-0.0691^{***} (0.0105)	ω	-0.0754^{***} (0.0110)	ω	-0.0731^{***} (0.0109)	ω	-0.0683^{***} (0.0105)
α	0.0459^{***} (0.0035)	α	0.0477^{***} (0.0037)	α	0.0472^{***} (0.0037)	α	0.0462^{***} (0.0036)
α^*	0.0393^{***} (0.0027)	α^*	0.0393^{***} (0.0027)	α^*	0.0394^{***} (0.0026)	α^*	0.0391^{***} (0.0027)
β	0.9853^{***} (0.0024)	β	0.9839^{***} (0.0025)	β	0.9844^{***} (0.0025)	β	0.9854^{***} (0.0024)
λ_0	-4.4735^{***} (0.4664)	λ_0	-4.4866^{***} (0.4762)	λ_0	-4.4852^{***} (0.4717)	λ_0	-4.4736^{***} (0.4707)
δ_1	0.5636^{***} (0.0862)	δ_1	0.9168^{***} (0.2072)	δ_1	0.9075^{***} (0.2088)	δ_1	0.5673^{***} (0.0866)
		γ_1	-0.6168^{***} (0.2390)	γ_1	-0.6062^{**} (0.2459)		
		κ_1	-0.0688^{**} (0.0284)	κ_1	-0.0691^{**} (0.0282)		
δ_2	-0.0789^{***} (0.0164)	δ_2	-0.0065 (0.0104)	δ_2	-0.0778^{***} (0.0164)	δ_2	-0.0575 (0.0451)
		γ_2	0.9181^{***} (0.1297)			γ_2	0.2599 (0.5359)
		κ_2	-0.0031 (0.0045)			κ_2	0.0125 (0.0096)
MDS (mean)	0.6780 (0.4103)	MDS (mean)	0.8230 (0.3643)	MDS (mean)	0.6228 (0.4300)	MDS (mean)	0.0059 (0.9386)
MDS (variance)	0.0017 (0.9671)	MDS (variance)	0.9797 (0.3223)	MDS (variance)	1.0579 (0.3037)	MDS (variance)	0.0017 (0.9672)
MDS (skewness)	0.3004 (0.5837)	MDS (skewness)	0.2770 (0.5987)	MDS (skewness)	0.3843 (0.5353)	MDS (skewness)	0.8657 (0.3521)
MDS (kurtosis)	0.9718 (0.3242)	MDS (kurtosis)	1.6887 (0.1938)	MDS (kurtosis)	1.6510 (0.1988)	MDS (kurtosis)	0.8814 (0.3478)
LL	3.3277	LL	3.3282	LL	3.3281	LL	3.3278
LR	7.6710 (0.1044)	LR	NA	LR	0.9277 (0.6288)	LR	5.8124 (0.0547)

Normal-inverse Gaussian (NIG) distribution; martingale difference sequence (MDS); log-likelihood (LL); likelihood-ratio (LR); not available (NA); realized volatility (RV); root mean squared error (RMSE); mean absolute error (MAE). *, **, and *** indicate significance at the 10, 5, and 1% levels, respectively. For the parameter estimates standard errors are reported in parentheses. For all other statistics of the table, p-values are reported in parentheses. The null hypothesis of the MDS test is the correctness of the NIG specification, which is checked up to the first four conditional moments. For the LR test, the most general model is the score-driven model for which all shape parameters are time-varying; the rest of the specifications are special cases, so the classical LR test can be used. Model specification: $y_t = \mu_t + \exp(\lambda_t)\epsilon_t$, $\epsilon_t \sim$NIG [0, 1, $\exp(\nu_t)$, $\exp(\nu_t)\tanh(\eta_t)$], $\mu_t = c + \phi\mu_{t-1} + \theta u_{\mu,t-1}$, and $\lambda_t = \omega + \beta\lambda_{t-1} + \alpha u_{\lambda,t-1} + \alpha^* \operatorname{sgn}(-\epsilon_{t-1})\,(u_{\lambda,t-1} + 1)$. For constant ν_t or η_t: $\nu_t = \delta_1$ and $\eta_t = \delta_2$. For dynamic ν_t or η_t: $\nu_t = \delta_1 + \gamma_1\nu_{t-1} + \kappa_1 u_{\nu,t-1}$ and $\eta_t = \delta_2 + \gamma_2\eta_{t-1} + \kappa_2 u_{\eta,t-1}$.

Table C3: Parameter estimates for the score-driven Skew-Gen-t models for the period of February 14, 1990 to October 21, 2021.

Constant τ_t, ν_t and η_t		Dynamic τ_t, ν_t and η_t		Dynamic τ_t, ν_t and constant η_t		Dynamic τ_t, constant ν_t and dynamic η_t	
c	0.0004*** (0.0001)	c	0.0005*** (0.0001)	C	0.0005*** (0.0001)	C	0.0005*** (0.0001)
ϕ	0.6348*** (0.1230)	ϕ	0.5875*** (0.1155)	Φ	0.5815*** (0.1252)	Φ	0.5672*** (0.1273)
θ	−0.0522*** (0.0139)	θ	−0.0710*** (0.0176)	Θ	−0.0706*** (0.0190)	Θ	−0.0725*** (0.0189)
ω	−0.0769*** (0.0114)	ω	−0.0821*** (0.0111)	ω	−0.0766*** (0.0114)	Ω	−0.0779*** (0.0116)
α	0.0462*** (0.0035)	α	0.0471*** (0.0036)	α	0.0466*** (0.0036)	α	0.0469*** (0.0037)
α^*	0.0390*** (0.0026)	α^*	0.0380*** (0.0025)	α^*	0.0394*** (0.0027)	α^*	0.0395*** (0.0026)
β	0.9849*** (0.0023)	β	0.9839*** (0.0023)	β	0.9850*** (0.0023)	β	0.9847*** (0.0024)
λ_0	−4.9494*** (0.4687)	λ_0	−4.9800*** (0.4745)	λ_0	−4.9428*** (0.4783)	λ_0	−4.9509*** (0.4782)
δ_1	−0.0637*** (0.0125)	δ_1	−0.0466 + (0.0290)	δ_1	−0.0469 + (0.0295)	δ_1	−0.0467 + (0.0292)
		γ_1	0.2428 (0.4289)	γ_1	0.2439 (0.4317)	γ_1	0.2482 (0.4256)
		κ_1	0.0113* (0.0064)	κ_1	0.0119* (0.0067)	κ_1	0.0121* (0.0065)
δ_2	2.1377*** (0.2837)	δ_2	0.8616 (1.3059)	δ_2	1.8314 (3.6328)	δ_2	2.1403*** (0.2826)
		γ_2	0.6651 (0.5057)	γ_2	0.1442 (1.6790)		
		κ_2	1.4759 (1.1459)	κ_2	0.7005 (0.9380)		
δ_3	0.4736*** (0.0433)	δ_3	0.0135* (0.0070)	δ_3	0.4742*** (0.0439)	δ_3	0.1903 (2.1881)
		γ_3	0.9690*** (0.0160)			γ_3	0.5988 (4.6118)
		κ_3	−0.0262** (0.0121)			κ_3	−0.0029 (0.0214)
MDS (mean)	1.6467 (0.1994)	MDS (mean)	0.0251 (0.8741)	MDS (mean)	0.0016 (0.9679)	MDS (mean)	0.0003 (0.9855)
MDS (variance)	0.0101 (0.9201)	MDS (variance)	0.2812 (0.5959)	MDS (variance)	0.1526 (0.6961)	MDS (variance)	0.0011 (0.9737)
MDS (skewness)	0.3501 (0.5541)	MDS (skewness)	0.7243 (0.3947)	MDS (skewness)	2.2946 (0.1298)	MDS (skewness)	1.6283 (0.2019)
MDS (kurtosis)	0.8544 (0.3553)	MDS (kurtosis)	0.5255 (0.4685)	MDS (kurtosis)	0.6189 (0.4315)	MDS (kurtosis)	0.8378 (0.3600)
LL	3.3292	LL	3.3299	LL	3.3294	LL	3.3294
LR	11.5992 (0.0715)	LR	NA	LR	7.9537 (0.0187)	LR	8.2267 (0.0164)

Skewed generalized t-distribution (Skew-Gen-t); martingale difference sequence (MDS); log-likelihood (LL); likelihood-ratio (LR); not available (NA); realized volatility (RV); root mean squared error (RMSE); mean absolute error (MAE). +, *, **, and *** indicate significance at the 15, 10, 5, and 1% levels, respectively. For the parameter estimates standard errors are reported in parentheses. For all other statistics of the table, p-values are reported in parentheses. The null hypothesis of the MDS test is the correctness of the Skew-Gen-t specification, which is checked up to the first four conditional moments. For the LR test, the most general model is the score-driven model for which all shape parameters are time-varying; the rest of the specifications are special cases, so the classical LR test can be used. Model specification: $y_t = \mu_t + \exp(\lambda_t)\epsilon_t$, $\epsilon_t \sim$ Skew-Gen-t[0, 1, $\tanh(\tau_t)$, $\exp(\nu_t) + 4$, $\exp(\eta_t)$], $\mu_t = c + \phi\mu_{t-1} + \theta u_{\mu,t-1}$, and $\lambda_t = \omega + \beta\lambda_{t-1} + \alpha u_{\lambda,t-1} + \alpha^* \operatorname{sgn}(-\epsilon_{t-1})\,(u_{\lambda,t-1} + 1)$. For constant τ_t, ν_t, or η_t: $\tau_t = \delta_1$, $\nu_t = \delta_2$, and $\eta_t = \delta_3$. For dynamic τ_t, ν_t, or η_t: $\tau_t = \delta_1 + \gamma_1\tau_{t-1} + \kappa_1 u_{\tau,t-1}$, $\nu_t = \delta_2 + \gamma_2\nu_{t-1} + \kappa_2 u_{\nu,t-1}$, and $\eta_t = \delta_3 + \gamma_3\eta_{t-1} + \kappa_3 u_{\eta,t-1}$.

Table C4: Parameter estimates for the score-driven Skew-Gen-*t* models for the period of February 14, 1990 to October 21, 2021.

Dynamic τ_t and constant ν_t, η_t		Constant τ_t and dynamic ν_t, η_t		Constant τ_t, dynamic ν_t and constant η_t		Constant τ_t, ν_t and dynamic η_t	
c	0.0005^{***} (0.0001)	c	0.0004^{***} (0.0001)	c	0.0008^{***} (0.0002)	C	0.0004^{***} (0.0001)
ϕ	0.5699^{***} (0.1270)	ϕ	0.6285^{***} (0.1116)	ϕ	0.2973 (0.2232)	Φ	0.6342^{***} (0.1229)
θ	-0.0719^{***} (0.0189)	θ	-0.0558^{***} (0.0133)	θ	-0.0564^{***} (0.0152)	Θ	-0.0523^{***} (0.0139)
ω	-0.0774^{***} (0.0115)	ω	-0.0804^{***} (0.0110)	ω	-0.0762^{***} (0.0113)	ω	-0.0771^{***} (0.0114)
α	0.0468^{***} (0.0036)	α	0.0464^{***} (0.0035)	α	0.0457^{***} (0.0036)	α	0.0463^{***} (0.0036)
α^*	0.0395^{***} (0.0026)	α^*	0.0375^{***} (0.0025)	α^*	0.0404^{***} (0.0026)	α^*	0.0390^{***} (0.0026)
β	0.9848^{***} (0.0023)	β	0.9842^{***} (0.0022)	β	0.9851^{***} (0.0023)	β	0.9849^{***} (0.0023)
λ_0	-4.9510^{***} (0.4773)	λ_0	-4.9785^{***} (0.4645)	λ_0	-4.9304^{***} (0.4731)	λ_0	-4.9480^{***} (0.4694)
δ_1	$-0.0471 + (0.0291)$	δ_1	-0.0649^{***} (0.0120)	δ_1	-0.0655^{***} (0.0128)	δ_1	-0.0638^{***} (0.0125)
γ_1	0.2446 (0.4234)						
κ_1	0.0120^{*} (0.0064)						
δ_2	2.1384^{***} (0.2791)	δ_2	0.7741 (1.0748)	δ_2	1.5597 (4.2769)	δ_2	2.1343^{***} (0.2875)
		γ_2	0.6975^{*} (0.4172)	γ_2	0.2558 (2.0233)		
		κ_2	1.5694 (1.1016)	κ_2	0.5141 (0.8756)		
δ_3	0.4744^{***} (0.0432)	δ_3	0.0137^{*} (0.0074)	δ_3	0.4782^{***} (0.0445)	δ_3	0.1959 (7.9114)
		γ_3	0.9687^{***} (0.0168)			γ_3	0.5868 (16.6857)
		κ_3	-0.0259^{**} (0.0125)			κ_3	-0.0008 (0.0210)
MDS (mean)	0.0005 (0.9822)	MDS (mean)	2.5162 (0.1127)	MDS (mean)	2.4570 (0.1170)	MDS (mean)	1.6559 (0.1982)
MDS (variance)	0.0048 (0.9445)	MDS (variance)	0.3499 (0.5542)	MDS (variance)	0.0942 (0.7589)	MDS (variance)	0.0082 (0.9280)
MDS (skewness)	1.6444 (0.1997)	MDS (skewness)	0.3362 (0.5620)	MDS (skewness)	0.4567 (0.4992)	MDS (skewness)	0.3521 (0.5529)
MDS (kurtosis)	0.6777 (0.4104)	MDS (kurtosis)	0.9899 (0.3198)	MDS (kurtosis)	0.0002 (0.9892)	MDS (kurtosis)	0.9030 (0.3420)
LL	3.3294	LL	3.3297	LL	3.3289	LL	3.3292
LR	8.2443 (0.0830)	LR	3.7653 (0.1522)	LR	16.5301 (0.0024)	LR	11.5976 (0.0206)

Skewed generalized *t*-distribution (Skew-Gen-*t*); martingale difference sequence (MDS); log-likelihood (LL); likelihood-ratio (LR); not available (NA); realized volatility (RV); root mean squared error (RMSE); mean absolute error (MAE). +, *, **, and *** indicate significance at the 15, 10, 5, and 1% levels, respectively. For the parameter estimates standard errors are reported in parentheses. For all other statistics of the table, *p*-values are reported in parentheses. The null hypothesis of the MDS test is the correctness of the Skew-Gen-*t* specification, which is checked up to the first four conditional moments. For the LR test, the most general model is the score-driven model for which all shape parameters are time-varying; the rest of the specifications are special cases, so the classical LR test can be used. Model specification: $y_t = \mu_t + \exp(\lambda_t)\,\epsilon_t$, $\epsilon_t \sim$Skew-Gen-$t[0, 1, \tanh(\tau_t), \exp(\nu_t) + 4, \exp(\eta_t)]$, $\mu_t = c + \phi\mu_{t-1} + \theta u_{\mu,t-1}$, and $\lambda_t = \omega + \beta\lambda_{t-1} + \alpha u_{\lambda,t-1} + \alpha^* \operatorname{sgn}(-\epsilon_{t-1})\,(u_{\lambda,t-1} + 1)$. For constant τ_t, ν_t, or η_t: $\tau_t = \delta_1$, $\nu_t = \delta_2$, and $\eta_t = \delta_3$. For dynamic τ_t, ν_t, or η_t: $\tau_t = \delta_1 + \gamma_1\tau_{t-1} + \kappa_1 u_{\tau,t-1}$, $\nu_t = \delta_2 + \gamma_2\nu_{t-1} + \kappa_2 u_{\nu,t-1}$, and $\eta_t = \delta_3 + \gamma_3\eta_{t-1} + \kappa_3 u_{\eta,t-1}$.

Appendix D

In this appendix, the circumstances of the extreme events that are referred to in Figure 4 are described. We highlight those days for which the degrees of freedom estimates $\exp(\nu_t) + 4 < 8$:

February 12 and 13, 1991. The Dow Jones industrial average, increased 71.54 points on February 11, 1991 (2.5 percent increase). The increase in the US stock market indices was motivated by (i) optimism on the Gulf War's outcome, and (ii) the confidence of the market that the moves by the Federal Reserve Board to bring interest rates down would pull the economy out of recession and restore consumer confidence.

November 18, 19, and 20, 1991. On November 15, 1991, the Dow Jones dropped 120.31 points. On November 15, 1991, The NASDAQ composite index declined 4.2% due to fears about the stability of the economy, a cap on credit-card interest rates and fading biotechnology shares.

December 24 and 31, 1991 and January 2, 1992. Beginning of the Japanese asset price bubble burst.

February 17, 1993. On February 16, 1993, the S&P 500 fell by 2.4%, due to higher taxes proposed by President Clinton.

May 19 and 22, 1995. Technology stocks moved lower due to potential tightening of monetary policy in the face of rising inflation.

June 24 and 25, 1997. In the end of June and beginning of July, investors deserted emerging Asian shares. Crashes occurred in Thailand, Indonesia, South Korea, and Philippines, reaching a climax in the 1997 mini-crash.

October 28, 29, and 30, 1997. Global stock market crash that was caused by an economic crisis in Asia. It is known as the 1997 mini-crash. On October 20, 1997, the US accused Microsoft of violating a pact to stop Microsoft forcing makers of personal computers to include its Internet browser automatically. On October 22, 1997, Compaq testified that Microsoft threatened to break the Windows 95 agreement if they showcased a Netscape icon. On October 27, 1997, Microsoft argued it should be "free from government interference". On October 29, 1997, Iraq's Revolution Command Council announced that it would no longer allow US citizens, and US aircraft to serve with UN arms inspection teams.

December 1, 1998. Severe losses in the US stock market caused by profit taking on excellent two-week performance by stocks. Downturn in European markets.

January 5, 6, and 7 and 10, 2000. The Nasdaq composite lowered, as investors reduced their positions in technology stocks and invested in basic industry and financial services companies. Moreover, the investors also have concerns of the possibility of higher interest rates. Later on March 2002, the collapse of the technology bubble took place.

February 28, March 1 and 2, 2007. Stock prices in the US declined 3.5%, after a 9% fall in the Shanghai market provoked worries worldwide about the global economy and the valuation of share prices. In the US, markets had already been shrinking due to concerns about deterioration in the mortgage market. Alan Greenspan told a conference on 26 February 2007 that a recession in the US was likely.

September 30, 2008. The US Congress rejected the Bush Administration's USD 700 billion Wall Street bailout plan, sending the Dow Jones industrial average down 778 points in a single day.

March 24, 2009. The Dow Jones lost 115 points (1.5%); the S&P 500 lost 17 points (2%); the Nasdaq composite lost 40 points (2.5%). Tecnology and bank shares led the selloff.

January 31, 2011. The Dow Jones Industrial Average declined 1.39% and closed at 11,823.70. The S&P 500 fell 1.79% and closed at 1,276.34. The Nasdaq slipped 2.48% and ended the day at 2,686.89. The CBOE Volatility Index (VIX) shot up 24.1% due to increased instability in the Middle East. Oil prices continued to trend higher due to the ongoing tensions in Egypt.

February 23, 2011. On February 11, 2011, Egyptian Revolution culminated in the resignation of Hosni Mubarak, and the transfer of power to the Supreme Military Council after 18 days of protests (Arab Spring). On 14 February 2011, the 2011 Bahraini uprising commenced. On 15 February 2011, Libyan protests began opposing Colonel Muammar al-Gaddafi's rule. Stocks declined as oil prices surged to briefly cross the USD 100 per barrel mark amid the mounting crisis in Libya.

August 9, 2011. On August 8, 2011 (also known as Black Monday 2011), US and global stock markets crashed, following the Friday night credit rating downgrade by Standard and Poor's of the US sovereign debt from AAA to AA+. On August 9, 2011, stocks ended with huge gains after the Federal Reserve announced that it will keep interest rates exceptionally low until 2013.

June 27, 28, and 29, 2016. On June 23, 2016, Brexit referendum, the United Kingdom voted to leave the European Union (EU). On June 24, 2016, British Prime Minister David Cameron resigned after the UK voted to leave the EU. On June 26, 2016, City of Falluja freed from Islamic State (IS) control after a month-long campaign by Iraqi forces. On June 28, 2016, suicide bombings and gun attacks at Istanbul's Ataturk Airport.

February 5, 6, and 7, 2018. On February 2, 2018, the S&P 500 fell by 2.1%, and it was followed by a fall of 4.1% on February 5, 2018. The uncertainty was motivated by a surge in interest rates, with the benchmark 10-year yield rising as much as 2.9% to hit a four-year high.

October 11 and 12, 2018. The Dow Jones Industrial Average (DJI) dropped 3.2%, to close at 25,598.74. The S&P 500 dropped 3.3% to close at 2,785.68. The Nasdaq Composite Index closed at 7,422.05, plummeting 4.1%. The fall was due to concerns of rapidly rising interest rates, a possible increase in the US inflation rate, and a slowing global growth.

February 25, 26 and 28, 2020. Global markets fell sharply amid fears that the COVID-19 was spreading. News reports that Italy and South Korea had more than 200 new cases fueled the sell-off. This crash was part of a worldwide recession caused by the COVID-19 pandemic.

June 12, 15, 16, and 17, 2020. The S&P 500 increased on June 12, 2020 by 1.3% and on June 16 by 1.9%. Investors are encouraged by the prospects of more reopenings, the Federal Reserve's expansion of its Main Street Lending Program, and the growing sentiment that the economy is reversing course toward expansion.

September 4, 8, 9, 10, and 11, 2020. Around those days, the S&P 500 was very volatile and exhibited the following changes: on September 3, 2020 a 3.5% fall, on September 8, 2020 a 2.8% fall, on September 9, 2020 a 2% increase, and on September 10, 2020 a 1.8% fall. The correction was mainly in the technological sector.

January 28, 2021. US stock markets closed sharply lower on the back of several weaker-than-expected quarterly earnings results. Investors' sentiment also took a hit after the Federal Reserve states in its latest policy statement that the pace of economic recovery has moderated.

References

Andersen, T. G., and T. Bollerslev. 1998. "Answering the Skeptics: Yes, Standard Volatility Models Do Provide Accurate Forecasts." *International Economic Review* 39 (4): 885–905.

Ayala, A., S. Blazsek, and A. Escribano. 2019. "Maximum Likelihood Estimation of Score-Driven Models with Dynamic Shape Parameters: An Application to Monte Carlo Value-At-Risk." In *Working Paper*, 19–2: University Carlos III of Madrid, Department of Economics. Also available at https://e-archivo.uc3m.es/handle/10016/28638.

Backus, D., M. Chernov, and I. Martin. 2011. "Disasters Implied by Equity Index Options." *Journal of Finance* 66 (6): 1969–2012.

Bakshi, G., N. Kapadia, and D. Madan. 2003. "Stock Return Characteristics, Skew Laws, and the Differential Pricing of Individual Equity Options." *The Review of Financial Studies* 16 (1): 101–43.

Basel Committee. 1996. "Supervisory Framework for the Use of "Backtesting" in Conjunction with the Internal Models Approach to Market Risk Capital Requirements." Also Available at www.bis.org.

Black, F. 1976. "Studies of Stock Market Volatility Changes." In *1976 Proceedings of the American Statistical Association Business and Economic Statistics Section*.

Blasques, F., S. J. Koopman, and A. Lucas. 2015. "Information-Theoretic Optimality of Observation-Driven Time Series Models for Continuous Responses." *Biometrika* 102 (2): 325–43.

Blasques, F., A. Lucas, and A. van Vlodrop. 2020. "Finite Sample Optimality of Score-Driven Volatility Models: Some Monte Carlo Evidence." *Econometrics and Statistics* 19: 47–57.

Blasques, F., J. van Brummelen, S. J. Koopman, and A. Lucas. 2022. "Maximum Likelihood Estimation for Score-Driven Models." *Journal of Econometrics* 227 (2): 325–46.

Blazsek, S., and L. A. Monteros. 2017. "Dynamic Conditional Score Models of Degrees of Freedom: Filtering with Score-Driven Heavy Tails." *Applied Economics* 49 (53): 5426–40.

Blazsek, S., H. C. Ho, and S. P. Liu. 2018. "Score-Driven Markov-Switching EGARCH Models: An Application to Systematic Risk Analysis." *Applied Economics* 50 (56): 6047–60.

Blazsek, S., A. Escribano, and A. Licht. 2022. "Score-Driven Location Plus Scale Models: Asymptotic Theory and an Application to Forecasting Dow Jones Volatility." *Studies in Nonlinear Dynamics & Econometrics*. https://doi.org/10.1515/snde-2021-0083.

Barndorff-Nielsen, O., and C. Halgreen. 1977. "Infinite Divisibility of the Hyperbolic and Generalized Inverse Gaussian Distributions." *Probability Theory and Related Fields* 38 (4): 309–11.

Bollerslev, T. 1986. "Generalized Autoregressive Conditional Heteroskedasticity." *Journal of Econometrics* 31 (3): 307–27.

Bollerslev, T. 1987. "A Conditionally Heteroscedastic Time Series Model for Speculative Prices and Rates of Return." *The Review of Economics and Statistics* 69 (3): 542–7.

Bollerslev, T., and V. Todorov. 2011. "Estimation of Jump Tails." *Econometrica* 79 (6): 1727–83.

Bollerslev, T., and V. Todorov. 2014. "Time-Varying Jump Tails." *Journal of Econometrics* 183 (2): 168–80.

Bollerslev, T., G. Tauchen, and H. Zhou. 2009. "Expected Stock Returns and Variance Risk Premia." *The Review of Financial Studies* 22 (11): 4463–92.

Bollerslev, T., V. Todorov, and L. Xu. 2015. "Tail Risk Premia and Return Predictability." *Journal of Financial Economics* 118 (1): 113–34.

Caivano, M., and A. C. Harvey. 2014. "Time-Series Models with an EGB2 Conditional Distribution." *Journal of Time Series Analysis* 35 (6): 558–71.

Christoffersen, P. 1998. "Evaluating Interval Forecasts." *International Economic Review* 39 (4): 841–62.

Cox, D. R. 1981. "Statistical Analysis of Time Series: Some Recent Developments." *Scandinavian Journal of Statistics* 8: 93–115.

Creal, D., S. J. Koopman, and A. Lucas. 2008. "A General Framework for Observation Driven Time-Varying Parameter Models." In *Discussion Paper 08-108/4*: Tinbergen Institute.

Creal, D., S. J. Koopman, and A. Lucas. 2011. "A Dynamic Multivariate Heavy-Tailed Model for Time-Varying Volatilities and Correlations." *Journal of Business & Economic Statistics* 29 (4): 552–63.

Creal, D., S. J. Koopman, and A. Lucas. 2013. "Generalized Autoregressive Score Models with Applications." *Journal of Applied Econometrics* 28 (5): 777–95.

Engle, R. F. 1982. "Autoregressive Conditional Heteroscedasticity with Estimates of the Variance of United Kingdom Inflation." *Econometrica* 50 (4): 987–1008.

Escanciano, J. C., and I. N. Lobato. 2009. "An Automatic Portmanteau Test for Serial Correlation." *Journal of Econometrics* 151 (2): 140–9.

Galbraith, J. W., and S. Zernov. 2004. "Circuit Breakers and the Tail Index of Equity Returns." *Journal of Financial Econometrics* 2 (1): 109–29.

Hansen, B. E. 1994. "Autoregressive Conditional Density Estimation." *International Economic Review* 35 (3): 705–30.

Hansen, P. R., and A. Lunde. 2006. "Consistent Ranking of Volatility Models." *Journal of Econometrics* 131 (1–2): 97–121.

Harvey, A. C. 2013. *Dynamic Models for Volatility and Heavy Tails*. Cambridge: Cambridge University Press.

Harvey, A. C., and T. Chakravarty. 2008. "Beta-t-(E)GARCH." In *Cambridge Working Papers in Economics 0840*. Cambridge: Faculty of Economics, University of Cambridge.

Harvey, A. C., and R. J. Lange. 2017. "Volatility Modeling with a Generalized *T*-Distribution." *Journal of Time Series Analysis* 38 (2): 175–90.

Harvey, A. C., and R. J. Lange. 2018. "Modeling the Interactions between Volatility and Returns Using EGARCH-M." *Journal of Time Series Analysis* 39 (6): 909–19.

Harvey, A. C., and G. Sucarrat. 2014. "EGARCH Models with Fat Tails, Skewness and Leverage." *Computational Statistics & Data Analysis* 76: 320–38.

Harvey, A. C., E. Ruiz, and N. Shephard. 1994. "Multivariate Stochastic Variance Models." *The Review of Economic Studies* 61 (2): 247–64.

Kelly, B., and H. Jiang. 2014. "Tail Risk and Asset Prices." *The Review of Financial Studies* 27 (10): 2841–71.

Kupiec, P. H. 1995. "Techniques for Verifying the Accuracy of Risk Measurement Models." *The Journal of Derivatives* 3 (2): 73–84.

Li, W. K. 2004. *Diagnostic Checks in Time Series*. Boca Raton: Chapman & Hall/CRC.

Liu, L. Y., A. J. Patton, and K. Sheppard. 2015. "Does Anything Beat 5-Minute RV? A Comparison of Realized Measures across Multiple Asset Classes." *Journal of Econometrics* 187 (1): 293–311.

Massacci, D. 2017. "Tail Risk Dynamics in Stock Returns: Links to the Macroeconomy and Global Markets Connectedness." *Management Science* 63 (9): 3072–89.

McDonald, J. B., and R. A. Michelfelder. 2017. "Partially Adaptive and Robust Estimation of Asset Models: Accommodating Skewness and Kurtosis in Returns." *Journal of Mathematical Finance* 7: 219–37.

Nelson, D. B. 1991. "Conditional Heteroskedasticity in Asset Returns: A New Approach." *Econometrica* 59 (2): 347–70.

Newey, K., and K. D. West. 1987. "A Simple, Positive Semi-definite, Heteroskedasticity and Autocorrelation Consistent Covariance Matrix." *Econometrica* 55 (3): 703–8.

Quintos, C., Z. Fan, and P. C. B. Phillips. 2001. "Structural Change Tests in Tail Behavior and the Asian Crisis." *The Review of Economic Studies* 68 (3): 633–63.

Schwaab, B., X. Zhang, and A. Lucas. 2020. ‘‘Modeling Extreme Events: Time Varying Extreme Tail Shape.’’ In Discussion Paper TI 2020-076/III. Tinbergen Institute.

Wooldridge, J. M. 1994. ‘‘Estimation and Inference for Dependent Processes.’’ In *Handbook of Econometrics*, vol. 4, edited by R. F. Engle and D. L. McFadden, 2639—738. Amsterdam: North-Holland.